PETROGENESIS AND TECTONO-MAGMATIC SIGNIFICANCE OF THE ALBANIDE - HELLENIDE SUBPELAGONIAN OPHIOLITES

Emilio Saccani*, Luigi Beccaluva*, Massimo Coltorti* and **Franca Siena***

* *Dipartimento di Scienze della Terra, Università di Ferrara, C.so E. I d'Este 32, 44100 Ferrara.*
Corresponding Author: Emilio Saccani, e-mail sac@unife.it.

Keywords: *Ophiolite, MORB, Supra-subduction, Albanide, Hellenide, Jurassic. Greece, Albania.*

ABSTRACT

The Mirdita-Subpelagonian ophiolites of the Albanide-Hellenide orogen are parts of a continuous belt extending from the former Yugoslavia to Greece, and share common geological, litho-stratigraphical, geochemical, and metallogenic features.

In the Albanian sector, two distinct ophiolitic belts can be clearly identified: the Western Belt, mainly composed of mid-ocean ridge (MORB) ophiolites, and the Eastern Belt characterized by supra-subduction zone (SSZ) ophiolites with prevalent island arc tholeiitic (IAT) and minor boninitic affinity. In the easternmost border of the Western Belt (Central Mirdita), a transitional zone with MORB/IAT intermediate basalts and boninitic dykes also occur.

In the Greek sector, a definite distinction into two ophiolitic belts cannot be made, and MORB-type ophiolites (western type) are subordinate, being represented only by the intrusive and lower volcanic sequences of the Pindos Massif. By contrast, SSZ- ophiolites (eastern type) are predominant and well-represented by the IAT and boninitic sequences of the Vourinos Massif, as well as by MORB/IAT intermediate basaltic-andesitic suites and boninites of the upper part of the Pindos volcanic sequence.

Petrological and geochemical modelling suggest that the different Albanide -Hellenide ophiolitic sequences originated from distinctly different parental magmas by partial melting of mantle sources progressively depleted by previous melt extractions. MORB may have derived from 10 - 20% partial melting of an undepleted lherzolitic source, while MORB/IAT intermediate basalts may have generated by ca. 10% of H_2O-assisted partial melting of a cpx-poor lherzolite that had previously experienced MORB extraction. IAT magmas and boninites may, in turn, have derived from 10 – 20 % and ca. 30% partial melting of the same source, variably enriched by subduction-derived fluids and related incompatible elements.

The favoured tectono-magmatic model for the genesis of the Albanide-Hellenide ophiolites implies a low plate-convergence velocity with: 1) intra-oceanic subduction within a pristine MORB lithosphere, resulting in SSZ magmatism with IAT affinity, and generation of a nascent arc by nearly open-system supply of undifferentiated basalts (sheeted dyke complexes); 2) progressive slab sinking and retreat coupled with mantle diapirism and extension from the arc axis to the forearc region, with generation of boninites and/or very low-Ti tholeiites from depleted sub-arc sources, leaving highly depleted harzburgitic residua; 3) contemporaneous generation at the spreading axis of IAT/MORB intermediate basalts resulting from the interference of MORB-source diapirs with suprasubduction mantle sources; 4) convergence processes leading to obduction of large and relatively intact lithospheric sections of SSZ ophiolites onto the Pelagonian continental margin, often with the interposition of metamorphic soles. The latter have prevalent MORB affinity and represent relics of the pristine MORB lithosphere overthrust by the still hot ophiolitic slab.

INTRODUCTION

Greek ophiolites have been the subject of research for a long time because they represent important elements for the reconstruction of the geodynamic evolution of the Hellenide orogenic belt. By contrast, Albanian ophiolites, though representing the most intact examples of Jurassic ophiolites in the Mediterranean region, have become accessible to the international scientific community only in the past decade.

Nonetheless, the increasing number of literature data from both Albanian (Mirdita) and Subpelagonian Greek ophiolites (Fig. 1) reveals that they share significant geological, geochemical and petrological characteristics (e.g. Hoeck et al., 2002; Beccaluva et al., 2004), suggesting a common tectono-magmatic evolution from the same oceanic basin.

The aim of this paper is to present a review of the petrogenesis and original tectonic setting of the Albanide-Hellenide Subpelagonian ophiolites (Fig. 1a) in the framework of the Mesozoic tectonic evolution of the Eastern Neo-Tethyan oceanic basin. For this purpose, attention has been focused on some key areas of the Albanide-Hellenide ophiolites, that is: the northern Mirdita (Fig. 1b) in Albania, and the Pindos (Fig. 1c) and Vourinos (Fig. 1d) Massifs in Greece. This review is based on published literature data, as well as on new data on mafic volcanic rocks, mainly from the northern Mirdita area.

REGIONAL TECTONIC SETTING

The Albanide-Hellenide orogenic belt is composed of several westward-verging tectono-stratigraphic zones, which can be referred to five fundamental paleo-tectonic settings (Beccaluva et al., 1997; Robertson and Shallo, 2000, Pe-Piper and Piper, 2002), from west to east: 1) the Adria continental margin (represented by five tectono-stratigraphic zones); 2) the Jurassic Subpelagonian ophiolitic domain; 3) the Pelagonian continental margin; 4) the Vardar ophiolitic domain; and 5) the Rhodope continental margin.

The tectono-stratigraphic zones, having different names in Albania and Greece, are (from west to east) the following.

The **Adria Continental Margin** includes:

The Sazani (in the Albanides)/pre-Apulian (in the Hellenides) Zone is dominated by Late Triassic-Jurassic to Cretaceous-Eocene platform carbonates, which are unconformably overlain by Early Miocene shallow marine to fluvial terrigenous deposits.

The Ionian Zone includes evaporites, Late Triassic-Early Jurassic shallow marine limestones and dolomites, and Jurassic-Eocene cherty limestones overlain by Oligocene flysch. The exposed successions of this zone record an Early to Middle Triassic rifting stage followed by a final break-up and Early Jurassic post-rift subsidence with deep-water sedimentation.

The Kruja (in the Albanides)/Gavrovo-Tripolitsa (in the

Hellenides) Zone in the Albanian sector is made up of Cretaceous-Eocene shallow-water limestones and dolomites, and Oligocene turbidites; the succession is locally covered by transgressive, Serravallian-Tortonian continental deposits. In the Greek sector, Triassic-Jurassic to Mid Cretaceous shallow-water carbonates are followed by Late Cretaceous deep-water carbonates and Late Eocene-early Miocene turbidites.

The Albanian Alps (in the Albanides)/Parnassus (in the Hellenides) Zone in the Albanian sector consists of two subzones (Valbona and Malesia-e-Madhe) with different paleogeographic and paleotectonic significance. The Valbona

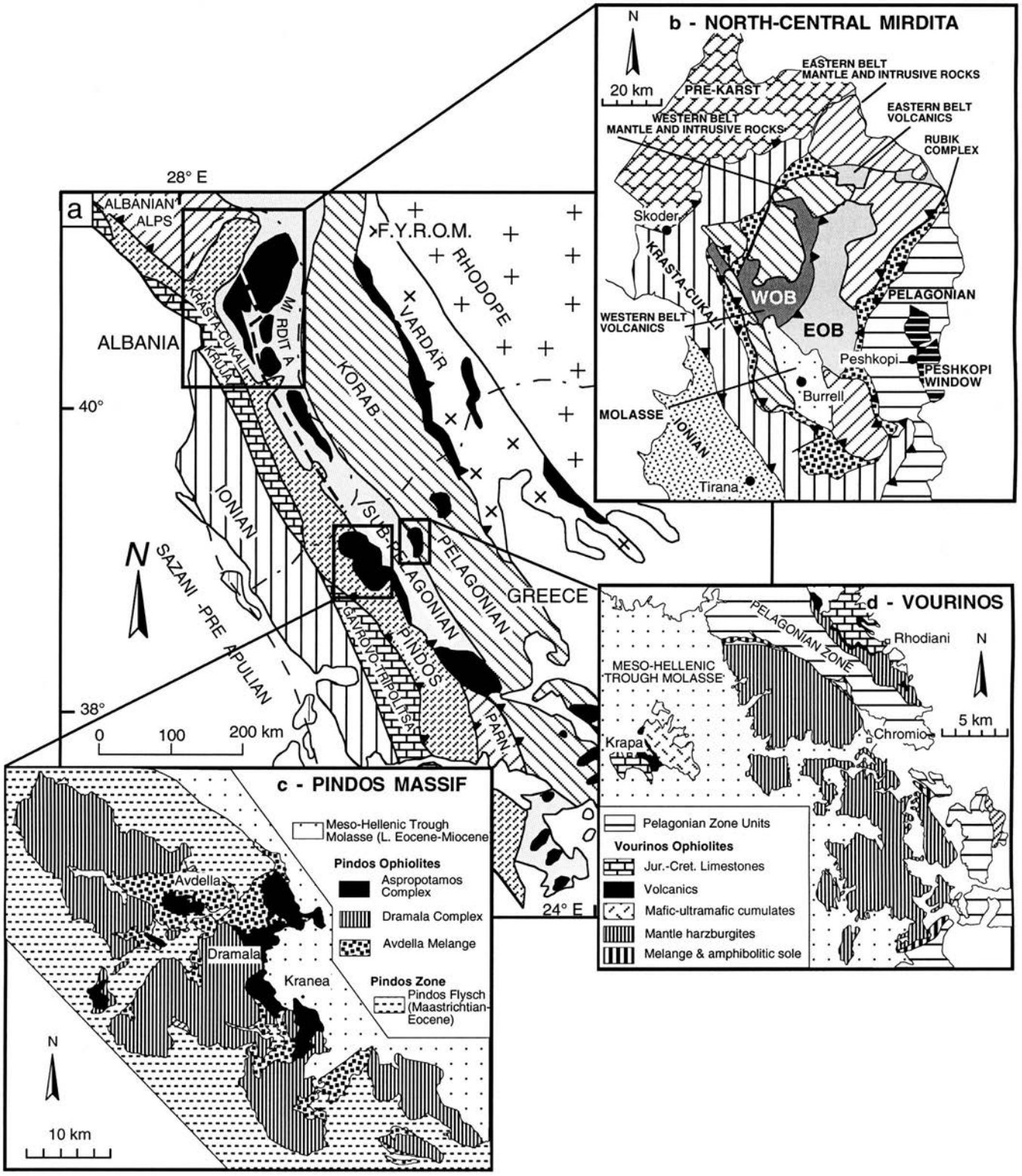

Fig. 1 - A: Simplified tectonic map of the Albanide-Hellenide area showing the main tectono-stratigraphic units. Compiled after Robertson (1994); Robertson and Shallo (2000) and references therein. Dashed line indicates the inferred boundary between the Eastern and Western Ophiolitic Belts (from Beccaluva et al., 1994). B: Simplified geological map of the northern Mirdita area. Modified from Bortolotti et al. (2002). WOB = western ophiolitic belt, EOB = eastern ophiolitic belt. C: Simplified geological map of the Pindos ophiolitic Massif. Modified from Jones and Robertson (1991). D: Simplified geological map of the Vourinos ophiolitic Massif. Modified from Moores (1969); Mavrides et al. (1982, 1991).

sub-zone is characterized by Jurassic limestones and Maastrichtian-Paleogene flysch, whereas the Malesia-e-Madhe sub-zone includes Late Triassic-Cretaceous limestones and Paleocene flysch. In Greece, the Parnassus zone has recently been interpreted as a microcontinental platform within the Neo-Tethyan ocean, and shows remarkable facies similarities with the Malesia-e-Madhe sub-zone (Robertson and Shallo, 2000).

The Krasta-Cukali (in the Albanides)/Pindos (in the Hellenides) Zone is composed of units representing the deep-water passive margin of the Adria, and showing significant facies variations from north to south. In the northern sector, the succession includes: Triassic mafic to intermediate volcanics, Triassic shales, limestones and radiolarian cherts, Jurassic carbonates and radiolarian cherts, early Cretaceous-Cenomanian carbonates, calcareous turbidites, mudstones, and marlstones. In the south Albanian sector, the succession is dominated by Cretaceous-Maastrichtian terrigenous turbidites and pelagic carbonates. In the Greek sector, the Pindos Zone is mainly characterized by Tithonian-Early Cretaceous deep-water limestones passing into Mid-Late Cretaceous pelagic carbonates and Late Cretaceous-Paleogene ophiolite-derived sandstones (Pindos Flysch).

The **Subpelagonian domain** is represented by Mirdita (in the Albanides)/Subpelagonian (in the Hellenides) Zone, which consists of Jurassic ophiolites and related sedimentary rocks. Ophiolites include sequences generated in both mid-ocean ridge (MORB) and in supra-subduction zone (SSZ) settings (Beccaluva et al., 1984, 1994; Shallo, 1994; Capedri et al., 1980 Bébien et al., 2000). However, in Albania, MORB and SSZ ophiolites are clearly represented by two distinct units (the western belt and eastern belt ophiolites, respectively) whereas, in Greece, a sharp geographical distinction cannot be made. The associated sedimentary rocks mainly include Triassic neritic carbonates and pelagic cherty limestones, radiolarian cherts at the top of the ophiolitic volcanics, and a supra-ophiolitic flysch. Sub-ophiolitic (Rubik Complex, Avdella Mélange, etc.) and supra-ophiolitic (Simoni Flysch) mélanges are widely associated to ophiolites in this Zone (Bortolotti et al., 1996).

The **Pelagonian continental margin** is represented by the Korab (in the Albanides)/Pelagonian (in the Hellenides) Zone, which are characterized by a Paleozoic basement consisting of an Ordovician-Devonian terrigenous sequence (with volcanic intercalations and granitoid intrusions) unconformably covered by a Permo-Triassic clastic sequence, possibly representing the early rifting stage of the Paleozoic continental domain. This sequence passes upwards to Early-Mid Triassic volcano-sedimentary sequences and Triassic-Jurassic neritic and pelagic carbonate deposits. Tertiary flysch and Triassic gypsum crop out in the Albanian Peshkopi tectonic window (Fig. 1b). In the Albanian - northern Greek sector, the Pelagonian Zone units were strongly deformed and metamorphosed during Late Jurassic-Cretaceous time, whereas in central and southern Greece the Pelagonian zone is unmetamorphosed.

The **Vardar** Zone represents the oceanic suture zone between the Pelagonian microplate and the Rhodope Massif, and includes a complex assemblage of Hercynian continental basement rocks, Jurassic ophiolites, deep-water sedimentary rocks, and calc-alkaline intrusives and volcanics (Bébien et al., 1984).

The **Rhodope** Massif consists of a pre-alpine continental basement showing a complex Mesozoic-Early Tertiary deformation history resulting from the northward collision of the Rhodope microcontinent with the Moesian platform (Robertson, 2002).

ANALYTICAL METHODS

Bulk rock major and trace element (Pb, Zn, Ni, Co, Cr, V, Rb, Sr, Ba, Nb, Zr) analyses were performed on pressed powder pellets using an automated Philips PW1400 X-ray fluorescence (XRF) spectrometer with the matrix correction methods proposed by Franzini et al. (1972). Precision and accuracy are better than 3% for Si, Ti, Ca, K and 7% for Al, Mn, Mg, Na, P, and are better than 10% for trace elements above 10 ppm. Volatiles were determined as loss on ignition (L.O.I.) at 1000°C.

Rare Earth Elements (REE), Sc, Y, Nb, Ta, Hf, Th, U were determined by inductively coupled plasma-mass spectrometry (ICP-MS), using a VG Elemental Plasma Quad PQ2 Plus at the Department of Earth Sciences of the University of Ferrara. Accuracy of better than 10% was evaluated using results for international standard rocks, duplicate runs of several samples, and the blind standards included in the sample set. ICP analyses were determined by inductively coupled plasma-optical emission spectrometry at the Centre de Recherches Pétrographique et Géochimique (C.R.P.G.) of Nancy (France) with an accuracy of 15% for Yb and Lu and better than 8% for other REE and Y (see analyses for reference standards from Roelandts and Michel, 1986).

MIRDITA OPHIOLITES

Geological framework

The Mirdita ophiolites extensively crop out from north to south Albania (Fig. 1a) covering an area ca. 250 km long and up to 70 km wide. They are associated throughout with the sub-ophiolitic mélange of the Rubik Complex with slices of metamorphic soles locally intercalated in-between. Ophiolites are overlain by a thick sedimentary sequence which, according to Bortolotti et al. (1996), can generally be subdivided in: 1) the Late Jurassic- Early Cretaceous ophiolite-derived sedimentary mélange (Mirdita Mélange) and Firza Flysch, and 2) the Early-Late Cretaceous post-orogenic, carbonate sequence.

The Rubik Complex consists of an assemblage of block and/or thrust sheets of (1) Triassic-Jurassic, mainly carbonate sequence, (2) Triassic basalts with intercalations of radiolarites, (3) serpentinized mantle peridotites, and (4) Late Jurassic - Early Cretaceous Mirdita Mélange and Firza Flysch (Bortolotti et al., 1996).

The metamorphic sole includes garnet-bearing amphibolites, garnet-bearing micaschists and paragneisses. Based on their geochemical signatures, the inferred protoliths for amphibolites are mid-ocean ridge basalts (MORB), cumulate gabbros and ocean island basalts, whereas paragneiss and micaschists probably represent siliciclastic sediments (Beccaluva et al., 1994; Carosi et al., 1996).

On the basis of petrographic, geochemical, and metallogenic data (Beccaluva et al., 1994; Shallo, 1994), the Albanian ophiolites can be subdivided into two NNW-SSE trending subparallel belts, the Western and the Eastern Ophiolitic Belts (Fig. 1a). The best exposed and preserved ophiolitic sequences of both Western and Eastern Belts are found in the northern Mirdita area (Fig. 1b).

Table 1 - Bulk-rock major and trace element analyses of selected basaltic rocks from the Mirdita Western Belt Ophiolites.

	MORB								MORB / IAT							
Locality	Kalur	Kalur	Porave	Blinish	Ungrej	Perlat	Blinish	Blinish	Ungrej	Kalur	Simon	Ungrej	Kalur	Kalur	Kaçinar	Kalur
Sample	RU273	RU269	AL127	AL50	RU192	SH42	AL4	AL5	RU200	RU274	RU122	RU199	RU280	RU268	RU124	RU283
Rock	Bas	Bas	Bas	Bas	Bas	Bas	Bas	Bas	Bas	Bas	Bas	Bas	Bas	Bas	Bas	Bas
Note	Pillow	Pillow	Pillow	Pillow	Pillow	Pillow	Pillow	Pillow	Pillow	Pillow	Pillow	MLF	Pillow	Pillow	Pillow	MLF
Data	(a)	(a)	(a)	(b)	(c)	(a)	(b)	(b)	(c)	(a)	(d)	(c)	(a)	(a)	(c)	(a)
XRF analyses:																
SiO_2	44.46	45.81	46.74	46.97	47.08	49.75	49.91	50.58	48.14	48.42	48.72	48.78	48.81	49.27	49.28	50.75
TiO_2	2.06	2.22	1.87	3.49	2.23	1.94	1.58	2.70	0.87	0.83	0.96	1.06	0.76	1.09	1.31	0.70
Al_2O_3	14.53	15.76	14.48	13.72	15.03	14.26	14.00	13.47	16.37	17.34	15.89	16.81	14.13	17.17	14.76	18.47
Fe_2O_3	1.33	1.85	1.63	2.09	1.83	1.77	1.45	1.89	1.35	1.11	1.38	1.25	1.30	1.21	1.38	1.03
FeO	8.89	12.35	10.89	13.90	12.17	11.78	9.64	12.59	9.04	7.37	9.19	8.32	8.67	8.10	9.23	6.87
MnO	0.18	0.22	0.18	0.25	0.21	0.20	0.17	0.20	0.17	0.18	0.18	0.20	0.20	0.18	0.16	0.16
MgO	6.26	6.97	8.46	5.11	7.13	6.65	7.79	4.87	8.08	7.56	8.65	7.66	8.52	6.79	8.92	6.08
CaO	11.43	10.17	8.97	8.06	8.17	9.20	10.74	6.42	11.25	12.94	10.97	13.22	13.91	10.97	11.24	10.44
Na_2O	1.81	2.69	2.90	3.74	3.88	2.23	3.43	5.46	2.92	1.43	2.50	2.24	1.94	2.89	2.80	3.15
K_2O	0.03	0.26	0.24	0.18	0.42	0.17	0.09	0.16	0.29	0.09	0.11	0.01	0.03	0.37	0.02	0.75
P_2O_5	0.16	0.18	0.28	0.32	0.15	0.16	0.14	0.25	0.09	0.03	0.09	0.15	0.01	0.07	0.12	0.03
L.O.I.	8.85	1.51	3.34	2.15	1.70	1.90	1.06	1.43	1.42	2.70	1.36	0.28	1.72	1.89	0.77	1.57
Total	100.00	100.00	100.00	100.01	100.00	100.01	100.00	100.00	100.00	100.00	100.00	100.00	100.00	100.00	99.99	100.00
mg#	55.6	50.2	58.1	39.8	51.1	50.4	59.3	41.1	61.4	64.6	62.6	62.1	63.7	59.9	63.3	61.2
Pb	n.a.	n.a.	21	n.a.	n.a.	n.a.	n.a.	n.a.	n.a.	n.a.	n.a.	n.a.	n.a.	n.a.	n.a.	n.a.
Zn	n.a.	n.a.	950	n.a.	n.a.	n.a.	n.a.	n.a.	n.a.	n.a.	n.a.	n.a.	n.a.	n.a.	n.a.	n.a.
Ni	81	62	70	44	76	37	63	43	87	89	67	108	117	103	63	69
Co	44	40	41	37	46	32	34	36	46	50	49	46	65	57	47	39
Cr	212	139	244	101	181	99	264	99	253	226	211	456	227	271	155	295
V	406	423	402	525	435	425	384	592	296	301	310	270	284	320	345	230
Rb	n.d.	n.d.	4	14	7	9	6	8	12	n.d.	5	7	n.d.	n.d.	12	n.d.
Sr	60	99	123	85	123	55	83	105	86	54	48	57	27	65	49	80
Ba	n.a.	n.a.	65	30	296	4	2	31	38	n.a.	33	43	n.a.	n.a.	22	n.a.
Nb	n.a.	n.a.	n.a.	n.d.	n.a.	2	3	5	n.a.	n.a.	n.a.	n.a.	n.a.	n.a.	n.a.	n.a.
Zr	107	116	124	209	133	91	82	156	53	13	52	91	11	27	111	14
ICP-MS and ICP analyses:																
	(*)	(*)	(*)	(°)	(*)	(°)	(°)	(°)	(*)	(*)	(*)	(*)	(*)	(*)	(*)	(*)
Sc	112	137	76.5	n.a.	94.4	n.a.	n.a.	n.a.	123	102	81.5	125	106	126	86.8	87.5
Y	38.6	46.6	35.5	84.6	53.0	47.8	39.7	60.9	27.3	17.1	24.9	30.0	18.2	26.8	33.3	17.5
La	3.69	2.60	4.62	5.06	3.29	3.15	2.70	6.25	0.43	0.27	0.46	0.70	0.35	0.70	1.25	0.32
Ce	11.9	9.39	13.8	21.1	11.4	11.1	8.46	18.7	1.69	1.27	1.88	2.91	1.34	2.47	4.42	1.27
Pr	2.25	1.88	2.40	n.a.	2.15	n.a.	n.a.	n.a.	0.39	0.31	0.45	0.63	0.29	0.55	0.95	0.33
Nd	12.8	10.5	13.3	21.2	12.7	10.7	8.42	15.2	2.70	2.30	3.46	3.84	2.08	3.53	6.25	2.33
Sm	4.57	4.08	4.75	9.03	4.94	4.83	3.83	6.19	1.39	1.29	1.97	1.68	1.20	1.86	2.88	1.28
Eu	2.46	1.64	1.63	3.18	1.63	1.51	1.38	2.03	0.64	0.64	0.80	0.79	0.58	0.85	1.09	0.63
Gd	5.64	5.39	5.96	11.8	5.79	6.03	5.02	7.68	2.20	1.94	2.71	2.41	1.95	2.81	3.71	2.02
Tb	1.15	1.13	1.17	n.a.	1.09	n.a.	n.a.	n.a.	0.51	0.46	0.56	0.53	0.46	0.62	0.71	0.44
Dy	7.08	7.18	7.94	13.1	7.13	7.56	5.79	8.83	3.46	3.19	3.93	3.57	3.26	4.18	4.75	3.00
Ho	1.58	1.63	1.66	n.a.	1.56	n.a.	n.a.	n.a.	0.83	0.76	0.85	0.85	0.78	0.98	1.01	0.71
Er	4.37	4.65	5.08	6.55	4.66	4.01	3.13	4.73	2.44	2.27	2.62	2.48	2.36	2.80	3.09	2.11
Tm	0.60	0.66	0.67	n.a.	0.61	n.a.	n.a.	n.a.	0.35	0.33	0.34	0.36	0.34	0.40	0.40	0.30
Yb	3.65	3.91	5.15	6.22	4.53	4.47	3.69	5.45	2.17	2.09	2.55	2.26	2.10	2.47	3.00	1.90
Lu	0.61	0.65	0.72	1.02	0.62	0.73	0.59	0.88	0.37	0.35	0.35	0.38	0.35	0.42	0.41	0.31
Nb	1.56	1.45	3.65	n.a.	1.88	n.a.	n.a.	n.a.	0.35	0.18	0.24	0.31	0.18	0.61	0.79	0.13
Hf	2.94	2.96	4.41	n.a.	3.49	n.a.	n.a.	n.a.	0.85	0.78	1.04	1.13	0.65	1.16	0.98	0.76
Ta	0.29	0.11	0.38	n.a.	0.12	n.a.	n.a.	n.a.	0.04	0.05	0.05	0.04	0.04	0.05	0.06	0.02
Th	0.10	0.09	0.38	n.a.	0.15	n.a.	n.a.	n.a.	0.03	0.01	0.02	0.02	0.01	0.08	0.08	0.01
U	0.03	0.05	0.37	n.a.	0.04	n.a.	n.a.	n.a.	0.01	0.02	0.00	0.01	0.09	0.04	0.01	0.04
Ti/V	30	31	28	40	31	27	25	27	18	16	19	24	16	20	23	18
Zr/Y	2.4	2.4	2.8	2.5	2.4	2.5	2.4	3.0	2.0	0.6	1.8	3.2	0.5	1.0	3.0	0.7
Ti/Cr	58	96	46	207	74	118	36	164	21	22	27	14	20	24	51	14
$(La/Sm)_N$	0.52	0.41	0.63	0.36	0.43	0.42	0.46	0.65	0.20	0.13	0.15	0.27	0.19	0.24	0.28	0.16
$(Sm/Yb)_N$	1.39	1.16	1.02	1.61	1.21	1.20	1.15	1.26	0.71	0.68	0.86	0.83	0.64	0.84	1.07	0.75
$(La/Yb)_N$	0.72	0.48	0.64	0.58	0.52	0.51	0.52	0.82	0.14	0.09	0.13	0.22	0.12	0.20	0.30	0.12

Abbreviations: Bas = basalt; MLF = massive lava flow; mg# = molar Mg/(Mg+Fe)*100; n.d. = not detected; n.a. = not analyzed. Data source: (a) original data, (b) Beccaluva et al. (1994); (c) Bortolotti et al. (2002); (d) Bortolotti et al. (1996). (*) ICP-MS analyses; (°) ICP analyses. Normalization values for REE ratios are from Sun and McDonough (1989).

Western Ophiolitic Belt

This belt is largely characterized by a stratigraphic sequence (Western Mirdita in Fig. 2) which includes, from bottom to top: (1) lherzolitic mantle tectonites; (2) a layered mafic-ultramafic cumulitic sequence, consisting of (pl-) dunites, troctolites, (pl-) wehrlites, (mela-) gabbros, and very scarce Fe-gabbros and plagiogranites; and (3) a volcanic sequence, which is mainly composed of pillow lava basalts with MORB (high-Ti) affinity (Beccaluva et al., 1994). The crystallization order observed in both intrusives and extrusives is olivine ± chromite followed by plagioclase and clinopyroxene, the order typical of MOR magmatism. All rock types are variably affected by ocean floor metamorphism mainly in greenschist facies. The most complete ophiolitic sequences of the Western Belt may reach a total thickness of about 3-4 km. Radiolarian cherts, overlying the western ophiolites display middle Bathonian assemblages (Marcucci et al., 1994).

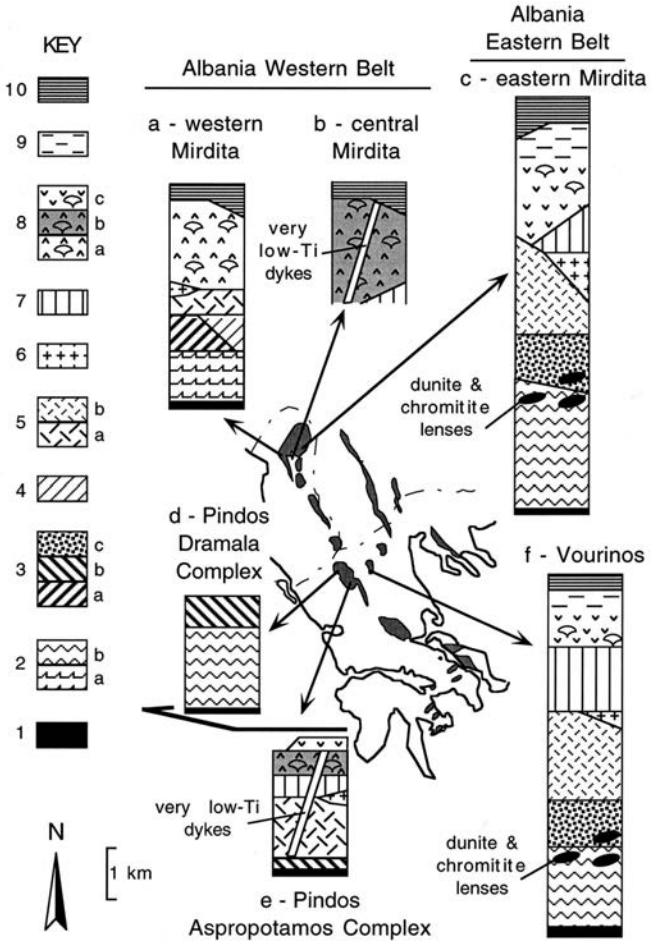

Fig. 2 - Stratigraphic columns of the main Jurassic ophiolitic types of Albania and Greece. Key. 1: Sub-ophiolitic mélange and metamorphic sole; 2: Mantle tectonites (a- lherzolite, b- harzburgite); 3: ultramafic cumulates (a- dunite, wehrlite, pl-dunite and pl-wehrlite; b- alternating sequences of dunite-anorthosite-troctolite-gabbro series and dunite-wehrlite-olivine gabbro series; c- dunite, chromitite, pl-lherzolite, lherzolite, olivine websterite, websterite); 4: troctolite; 5: mafic cumulates (a- gabbro; b- gabbronorite); 6: Qz-diorite and plagiogranite; 7: sheeted dykes; 8: mafic pillowed and massive volcanics (a- high-Ti basalts; b- alternating high-Ti and MORB/IAT intermediate basalts; c- low-Ti and very low-Ti volcanics and dykes); 9: andesite, dacites, rhyolite volcanics and dykes; 10: sedimentary sequences including radiolarian cherts and flysch. Compiled from: Jones and Robertson (1991); Beccaluva et al. (1994, 1997); Bortolotti et al. (1996, 2002); Robertson (2002); Saccani and Photiades (2004).

The eastern part of this belt (central Mirdita in Fig. 2) is characterized by the occurrence of volcanic sequences where pure MORBs alternate with basalts showing MORB / island arc thoeliite (IAT) intermediate geochemical features, and are cross-cut by very low-Ti basaltic dykes with boninitic affinity (Bortolotti et al., 1996, 2002, Bébien et al., 2000; Hoeck et al., 2002). Moreover, these sequences locally show sheeted dyke complexes at their base.

The geochemical characteristics of basaltic rocks showing pure MORB affinity (high-Ti) are typified by relatively high TiO_2 content (>1.30wt%) and Ti/V ratios (24-41). Accordingly, in the discrimination diagram of Fig. 3, they cluster in the field for basalts generated at mid-ocean ridge settings (Shervais, 1982; Beccaluva et al., 1983). High-Ti basalts from the Mirdita display relatively abundant high field strength element (HFSE) concentrations (HFSE / N-MORB = 1 to 5), 20 to 50 times chondritic abundances for heavy REE (HREE) (Fig. 4a) and significant light REE (LREE) depletion (La_N/Sm_N = 0.36-0.63; La_N/Yb_N = 0.48-0.72) (Bortolotti et al., 1996, 2002; Hoeck et al., 2002). All these characteristics are consistent with N-MORB compositions at variable degrees of differentiation, as suggested by FeO_t, TiO_2, and V enrichments, typical of low-P, tholeiitic fractionation at a mid-ocean ridge (Beccaluva et al., 1994, Bortolotti et al., 1996, 2002; Bébien et al., 2000; Hoeck et al., 2002).

The MORB / IAT intermediate basalts of central Mirdita (medium-Ti basalts of Bortolotti et al., 2002; low Zr/Y basalts of Hoeck et al., 2002) show TiO_2 contents varying from 0.71 wt% to 1.32 wt%, Zr = 11-111 ppm, Y = 21-37 ppm, and P_2O_5 = 0.01 wt% - 0.15 wt%. These intermediate geochemical features are evidenced in the Ti vs. V discrimination diagram (Fig. 3), where they cluster across the boundary between the IAT and MORB fields (Ti/V = 20), as well as by the HFSE depletion intermediate between the Western belt N-MORBs and the Eastern Belt IATs (0.5 to 1 times N-MORB: Bortolotti et al., 1996, 2002, Hoeck et al., 2002). These basalts are characterized by severe Th and LREE depletion (La_N/Sm_N = 0.15-0.28). Co, Ni, and Cr contents, usually higher than those of MORBs, suggest that these basalts represent rather primitive magmas.

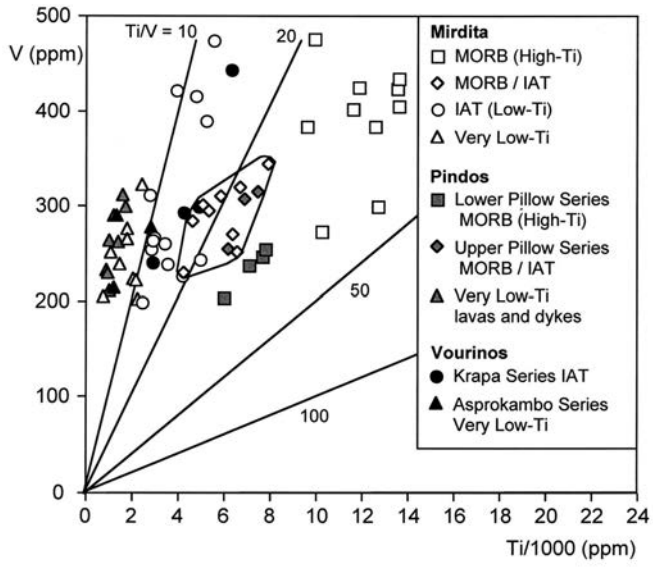

Fig. 3 - V vs. Ti/1000 discrimination diagram (Shervais, 1982) for mafic volcanic and subvolcanic rocks from the Mirdita, Pindos, and Vourinos ophiolites. Field encircles MORB/IAT intermediate basalts from different localities.

Very low-Ti basaltic dykes, sporadically found in the central Mirdita, display boninitic affinities and geochemical characteristics undistinguishable from similar lithologies of the Eastern Belt (e.g. sample RU196 in Table 2).

Eastern Ophiolitic Belt

The eastern ophiolitic belt shows a generalized sequence that is distinctly different from those of the Western Belt (Beccaluva et al., 1994; 1997) and includes (Eastern Mirdita in Fig. 2), from bottom to top: (1) harzburgitic mantle tectonites with dunite and chromitite pods and lenses in their upper part; (2) ultramafic cumulates consisting of dunites with chromitite layers, (ol-) websterites, and plagioclase-lherzolites with very subordinate troctolites in few-decimetre layers in the lower part of the cumulitic sequences of the Bulqiza and Shebenik ultramafic massifs (Beccaluva et al., 1994; Bébien et al., 1998); (3) mafic cumulates mainly composed of (ol-) gabbronorites, followed by abundant quartz-diorites and plagiogranites; (4) a sheeted dike complex; (5) a volcanic sequence including massive and pillowed basalts, basaltic andesites, andesites, dacites and rhyolites showing mainly IAT (low-Ti), and subordinately, boninitic (very low-Ti) affinities (Beccaluva et al., 1994; Shallo, 1994; Bébien et al., 2000; Bortolotti et al., 1996). Boninitic rocks are also found as dykes cutting the whole ophiolitic sequence. The crystallization order is olivine ± chromite, pyroxene, followed by plagioclase, magnetite, ilmenite and, finally, hornblende in quartz-diorites and plagiogranites. The most complete ophiolitic sequences of the Eastern Belt are characterized by a total thickness (from mantle tectonites to volcanics) of about 6-8 km.

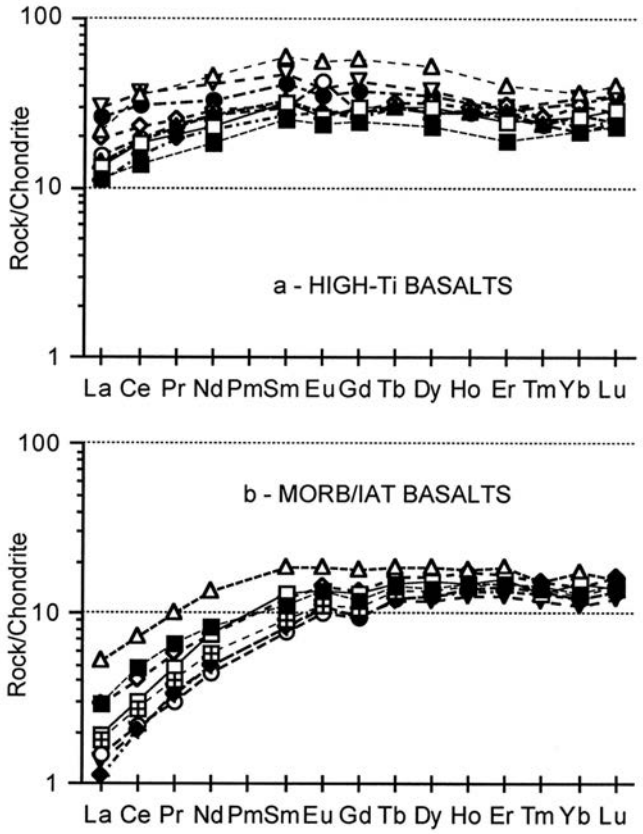

Fig. 4 - Chondrite-normalized (Sun and McDonough, 1989) REE patterns for basalts from the Mirdita Western Belt Ophiolites. A: high-Ti basalts; B: MORB/IAT intermediate basalts.

The radiolarian cherts topping the eastern belt ophiolites display ages similar to those of the western ophiolites, ranging from middle Bathonian at the base to middle Bathonian - early Callovian at the top (Marcucci et al., 1994; Marcucci and Prela, 1996).

IAT basaltic rocks range in TiO_2 from 0.29 wt% to 0.81 wt%, (Table 2) and in Ti/V ratios between 10 and 20 (Fig. 3). N-MORB normalized HFSE patterns range from 0.2 to 0.8 (Bortolotti et al., 2002). Low-Ti basaltic - andesitic rocks are characterized by depletion in LREE (Fig. 5a, b), as exemplified by the La_N/Sm_N and La_N/Yb_N ratios ranging from 0.15 to 0.64 and 0.11-0.56, respectively, whereas HREE are significantly more depleted (6 to 15 times chondritic abundances) when compared to the Western Belt MORBs.

Very low-Ti basalts and basaltic andesites resembling high-Ca boninites (Crawford et al., 1989) and are typically characterized by very low TiO_2 contents (0.12-0.39 wt%), coupled with high amounts of MgO (9.62-16.72 wt%) and CaO (9.87-11.91 wt%). Ti/V ratios are less than 10 (Fig. 3) typical of boninitic-type mafic rocks. Basalts and basaltic andesites are generally characterized by a severe HFSE and REE depletion (Table 2); REE patterns display both LREE depleted (Fig. 5c) and U-shaped (Fig. 5d) chondrite-normalized patterns.

PINDOS OPHIOLITES

Geological framework

The Pindos Massif (Fig. 1c) represents the widest ophiolitic outcrop of the Hellenides (2500 km^2). It is characterized by ophiolitic successions dismembered in a series of west-verging, thrust sheets imbricated together with platform carbonates, pelagic and turbiditic sediments and mélange units. These thrust sheets are emplaced over the autochthonous Maastrichtian-Eocene Pindos Flysch (Fig. 1c). According to Jones and Robertson (1991), the Jurassic Pindos Ophiolite Group represents the uppermost tectonic element in the Pindos Massif, and it can be subdivided into two main tectonic units (from bottom to top): the Aspropotamos Complex and the Dramala Complex (Figs.1c, 2). Both these units are characterized by a metamorphic sole (Loumnitsa Unit) and a sub-ophiolitic mélange (Avdella Mélange) at their base. The Pindos ophiolite Group is overlain by the Eocene-Miocene molasse deposits of the Meso-Hellenic Trough (Fig. 1c).

The Aspropotamos Complex, although highly dismembered, shows an apparent stratigraphic sequence (Fig. 2) including: layered ultramafic and mafic cumulates, as well as isotropic mafic intrusive and mafic volcanic rocks (Montigny et al., 1973). The ultramafic-mafic cumulates are characterized by alternating sequences of (1) dunite-anorthosite-troctolite-gabbro and (2) dunite-wehrlite-olivine gabbro, passing upward into isotropic gabbros and scarce plagiogranites.

A sheeted dyke complex marks the transition between the intrusive and volcanic sequence; the latter consists of pillow and massive basalts, basaltic breccias and hyaloclastites. The mafic rocks of the Aspropotamos Complex display the coexistence of distinct magmatic affinities. In fact, in the intrusive section, the sequences dunite-anorthosite-troctolite-gabbro may have resulted from a fractional crystallization order Ol, Pl, Cpx typical of MOR-type magmatism; in contrast, the sequences dunite-wehrlite-

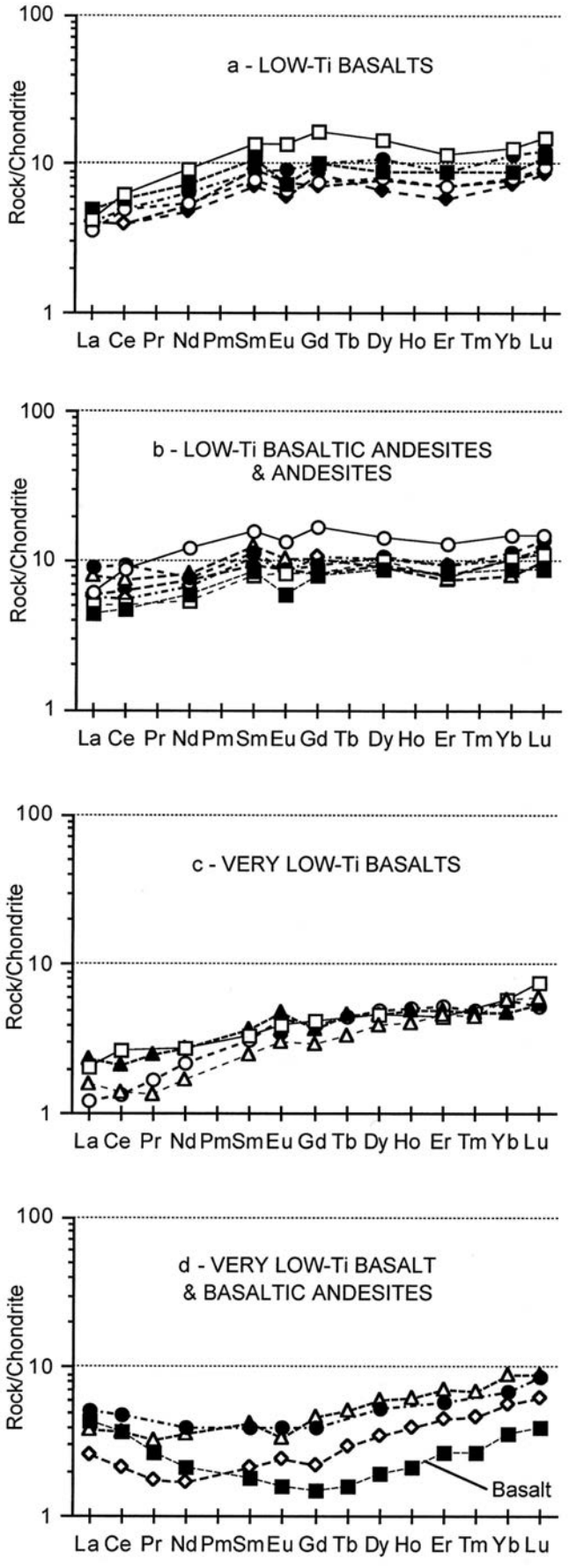

Fig. 5 - Chondrite-normalized (Sun and McDonough, 1989) REE patterns for volcanic and subvolcanic rocks from the Mirdita Eastern Belt Ophiolites. a: low-Ti basalts; b: low-Ti basaltic andesites and andesites; c: very low-Ti basalts; d: very low-Ti basalts and basaltic andesites.

olivine gabbro reflect a Ol, Cpx, Pl-Opx fractional crystallization order, typical of supra-subduction zone-type magmatism (Beccaluva et al., 1983).

Accordingly, in the volcanic sequence, Capedri et al. (1980) provided evidence for the presence of both MORBs and IAT volcanics cut by boninitic dykes in the Metsovo area. Kostopoulos (1988) documented the occurrence of volcanic sequences in the central sector of Pindos, in which rocks with different magmatic affinities alternate, thus reflecting a general evolution from MORB to IAT, and finally to boninitic rocks. In addition, Saccani and Photiades (2004) reported a volcanic sequence in the Aspropotamos river area consisting of (from bottom to top): 1) a lower pillow lava with MORB (high-Ti) affinity; 2) lava flows showing boninitic (very low-Ti) affinity; 3) an upper pillow lava section with MORB/IAT intermediate basalts; and 4) boninitic dykes cutting the whole sequence.

The Dramala Complex is mainly composed (Fig. 2) of variably serpentinized harzburgitic tectonites locally covered by dunite, pyroxenite and ultramafic cumulates (Jones and Robertson, 1991).

The Loumnitsa Unit represents the metamorphic sole of both Aspropotamos and Dramala Complexes (Fig. 1c, 2), and consists of metabasites and metasedimentary rocks ranging from greenschist to amphibolite facies. According to Jones and Robertson (1991), two main types of mafic protoliths are found in this Unit: typical mid-ocean ridge basalts (MORBs) and within-plate basalts (WPBs). Various dating methods (Thuizat et al., 1981; Spray et al., 1984 and references therein) give ages ranging from 163±3Ma to 172±5Ma.

The Avdella Mélange is a typical tectono-sedimentary mélange (Kemp and McCaig, 1984; Jones and Robertson, 1991), which occurs at the base of both Aspropotamos and Dramala Complexes. Blocks in the mélange include sedimentary rocks, basalts, rocks of the metamorphic sole, as well as radiolarian cherts indicating both Late Triassic and Jurassic ages. The available analyses on basaltic blocks reveal MORB and WPB compositions typical of oceanic-ridge and oceanic island settings, respectively (Jones and Robertson, 1991).

Geochemistry

Saccani and Photiades (2004) recognized three main geochemical groups in the volcanic sequence of the Aspropotamos River section: (1) high-Ti basalts from the lower part of the pillow sequence; (2) MORB/IAT intermediate basalts and basaltic andesites from the upper part of the pillow sequence; and (3) very low-Ti basaltic and basaltic andesitic dykes and massive lava flows intercalated in the pillow sequence. These groups can be identified in the V *vs.* Ti discrimination diagram of Fig. 3, where basaltic rocks from the lower pillow sequence display Ti/V ratios typical of MORBs (around Ti/V = 30); the upper pillow sequence has lower Ti/V ratios (22), and dykes and massive lava flows exhibit Ti/V ratios comparable with those of boninitic rocks (lower than 10).

High-Ti basalts from the lower pillow sequence are characterized by HFSE concentrations approximately equal to N-MORB, and rather flat chondrite-normalized REE patterns (Fig. 6a) with a mild LREE depletion ($La_N/Sm_N = 0.89$).

Volcanics from the upper pillow have very low Ni and Cr contents (11-12 ppm, 16-19 ppm, respectively), moderate to low MgO (4.1-7.59%), and higher FeO_t/MgO ratio (1.4-

Table 2 - Bulk-rock major and trace element analyses of selected volcanic and subvolcanic rocks from the Mirdita Eastern Belt Ophiolites.

	IAT								VERY LOW-Ti							
Local.	Kalivar	G.Vogel	Kalivar	Perlat	Kalivar	Tuc	Puke	Q.Mali	Gjazuj	Shemri	Tuç	Ungrej	Tuc	Arst	Arst	Kalivar
Sample	A266	AL48	A261	A432	A256	A462	SH47	AL40	IA204	IA144	AL139	RU196	A464	AL130	AL129	A257
Rock	Bas	Bas Pillow	Bas	Bas	Bas	B.And	B.And	And Dyke	Bas	Bas	Bas Pillow	Bas Dyke(1)	B.And	B.And Dyke	B.And Dyke	B.And
Note																
Data	(a)	(a)	(b)	(b)	(b)	(b)	(b)	(a)	(a)	(a)	(a)	(c)	(b)	(a)	(a)	(b)
XRF analyses:																
SiO_2	47.92	48.54	51.66	51.92	52.88	54.54	54.70	57.62	47.68	50.14	51.54	52.07	52.71	54.81	55.32	56.57
TiO_2	0.62	0.81	0.89	0.44	0.46	0.76	0.58	0.66	0.33	0.12	0.29	0.35	0.29	0.39	0.18	0.24
Al_2O_3	15.66	14.60	14.23	14.64	13.67	13.42	15.10	13.58	12.01	9.41	14.40	12.38	14.61	15.10	10.46	14.01
Fe_2O_3	1.47	1.25	1.45	1.13	1.34	1.39	1.34	1.44	1.11	1.28	1.20	1.07	1.16	1.34	1.03	1.05
FeO	9.79	8.33	9.65	7.50	8.93	9.26	8.90	9.61	7.42	8.52	8.01	7.15	7.76	8.94	6.89	7.32
MnO	0.11	0.16	0.15	0.13	0.18	0.14	0.17	0.11	0.15	0.20	0.14	0.15	0.13	0.15	0.14	0.16
MgO	6.68	10.70	6.90	9.84	10.88	7.74	7.11	6.30	16.11	16.31	9.38	12.02	9.49	5.57	11.77	7.99
CaO	8.37	12.92	8.02	9.13	3.34	4.50	5.07	2.75	11.02	11.07	11.62	10.92	9.53	7.69	10.57	4.73
Na_2O	4.35	1.39	3.81	1.66	3.46	2.94	3.60	5.78	1.51	0.42	0.59	2.22	0.73	3.03	1.75	5.68
K_2O	0.02	0.03	0.01	0.07	0.03	1.25	0.80	0.04	0.04	0.03	0.10	0.04	0.08	0.05	0.12	0.02
P_2O_5	0.06	0.11	0.10	0.08	0.06	0.06	0.05	0.05	0.06	0.05	0.24	0.03	0.07	0.11	0.20	0.04
L.O.I.	4.94	1.15	3.14	3.45	4.78	3.99	2.58	2.04	2.57	2.46	2.48	1.60	3.43	2.82	1.57	2.19
Total	99.99	100.00	100.01	99.99	100.01	99.99	100.01	100.00	100.00	100.00	100.00	100.00	100.00	100.00	100.00	100.00
mg#	55.1	69.8	56.3	70.2	68.7	60.1	58.7	54.1	79.5	77.3	67.6	75.0	68.5	52.6	75.3	65.8
Pb	n.a.	n.a.	n.a.	n.a.	n.a.	n.a.	n.a.	n.a.	5	4	3	n.a.	n.a.	9	2	n.a.
Zn	n.a.	n.a.	n.a.	n.a.	n.a.	n.a.	n.a.	n.a.	57	32	72	n.a.	n.a.	84	82	n.a.
Ni	21	86	49	53	54	24	23	10	242	370	146	160	89	22	116	33
Co	34	46	41	35	26	28	28	34	54	63	42	41	38	33	38	31
Cr	49	482	45	114	161	50	66	20	878	1702	563	734	294	38	777	113
V	422	244	474	312	264	416	321	337	224	205	276	223	266	323	252	240
Rb	n.d.	n.d.	n.d.	n.d.	4	9	15	n.d.	10	14	6	n.d.	n.d.	2	2	n.d.
Sr	91	42	19	85	39	81	77	36	950	25	27	117	34	8	79	27
Ba	27	22	9	29	11	29	61	42	170	18	64	334	23	30	57	18
Nb	n.d.	n.d.	n.d.	n.d.	n.d.	n.d.	n.d.	n.d.	n.a.	n.a.	n.a.	n.a.	n.d.	n.a.	n.a.	n.d.
Zr	21	34	43	28	36	34	21	31	50	15	12	36	12	30	27	19
ICP-MS and ICP analyses:																
	(°)	(°)	(°)	(°)	(°)	(°)	(°)	(°)	(*)	(*)	(*)	(*)	(°)	(*)	(*)	(°)
Sc	n.a.	n.a.	n.a.	n.a.	n.a.	n.a.	n.a.	n.a.	94.7	76.4	81.2	116	n.a.	77.7	80.2	n.a.
Y	11.4	22.7	19.3	11.9	13.9	16.8	16.3	17.6	9.46	3.84	7.07	9.41	8.05	10.3	5.27	9.00
La	0.96	1.01	0.98	0.96	0.86	1.20	1.42	2.11	0.29	1.03	0.37	0.56	0.48	0.90	0.61	1.21
Ce	2.42	3.77	3.06	2.44	3.05	3.09	3.83	5.64	0.82	2.27	0.85	1.29	1.66	2.27	1.31	2.89
Pr	n.a.	n.a.	n.a.	n.a.	n.a.	n.a.	n.a.	n.a.	0.16	0.25	0.13	0.24	n.a.	0.31	0.16	n.a.
Nd	2.50	4.33	3.03	2.27	2.58	2.49	3.49	3.64	1.03	0.98	0.78	1.30	1.27	1.66	0.79	1.82
Sm	1.42	2.07	1.34	1.10	1.21	1.21	1.41	1.72	0.49	0.28	0.38	0.57	0.51	0.66	0.33	0.61
Eu	0.44	0.78	0.54	0.35	0.39	0.47	0.51	0.51	0.25	0.09	0.18	0.28	0.23	0.19	0.14	0.23
Gd	1.46	3.42	2.10	1.74	1.57	1.69	1.67	1.95	0.80	0.30	0.61	0.76	0.87	0.95	0.45	0.82
Tb	n.a.	n.a.	n.a.	n.a.	n.a.	n.a.	n.a.	n.a.	0.17	0.06	0.13	0.17	n.a.	0.19	0.11	n.a.
Dy	2.00	3.67	2.71	1.71	2.04	2.56	2.41	2.68	1.25	0.48	1.00	1.17	1.17	1.52	0.89	1.35
Ho	n.a.	n.a.	n.a.	n.a.	n.a.	n.a.	n.a.	n.a.	0.29	0.12	0.23	0.28	n.a.	0.36	0.22	n.a.
Er	1.16	1.92	1.49	0.95	1.19	1.26	1.31	1.54	0.89	0.44	0.78	0.82	0.74	1.18	0.74	0.96
Tm	n.a.	n.a.	n.a.	n.a.	n.a.	n.a.	n.a.	n.a.	0.13	0.07	0.11	0.12	n.a.	0.18	0.12	n.a.
Yb	1.33	2.15	1.93	1.24	1.36	1.74	1.74	1.91	0.99	0.60	0.98	0.82	1.00	1.50	0.97	1.18
Lu	0.23	0.38	0.31	0.22	0.24	0.28	0.31	0.35	0.14	0.10	0.15	0.14	0.19	0.23	0.16	0.22
Nb	n.a.	n.a.	n.a.	n.a.	n.a.	n.a.	n.a.	n.a.	0.35	0.92	0.22	0.58	n.a.	0.46	0.54	n.a.
Hf	n.a.	n.a.	n.a.	n.a.	n.a.	n.a.	n.a.	n.a.	0.36	0.35	0.33	0.42	n.a.	0.63	0.45	n.a.
Ta	n.a.	n.a.	n.a.	n.a.	n.a.	n.a.	n.a.	n.a.	0.05	0.30	0.03	0.09	n.a.	0.05	0.06	n.a.
Th	n.a.	n.a.	n.a.	n.a.	n.a.	n.a.	n.a.	n.a.	0.03	0.52	0.10	0.08	n.a.	0.26	0.15	n.a.
U	n.a.	n.a.	n.a.	n.a.	n.a.	n.a.	n.a.	n.a.	0.01	0.24	0.08	0.03	n.a.	0.12	0.06	n.a.
Ti/V	9	20	11	8	10	11	11	12	9	3	6	10	7	7	4	6
Zr/Y	1.3	1.7	1.9	2.0	2.2	1.7	1.6	1.8	5.6	5.2	1.5	3.4	1.2	2.5	4.5	1.7
Ti/Cr	77	10	119	23	17	90	53	197	2		3	3	6	61	1	13
$(La/Sm)_N$	0.44	0.31	0.47	0.56	0.46	0.64	0.65	0.79	0.38	2.37	0.63	0.64	0.61	0.89	1.20	1.28
$(Sm/Yb)_N$	1.19	1.07	0.77	0.99	0.99	0.77	0.90	1.00	0.55	0.51	0.44	0.77	0.57	0.48	0.38	0.57
$(La/Yb)_N$	0.52	0.34	0.36	0.56	0.45	0.49	0.59	0.79	0.21	1.22	0.27	0.49	0.34	0.43	0.45	0.74

(1) Dyke in Western Ophiolitic Belt MORBs.

Abbreviations: Bas = basalt; B.And = basaltic andesite; And = andesite; mg# = molar Mg/(Mg+Fe)*100; n.d. = not detected; n.a. = not analyzed. Data source: (a) original data, (b) Beccaluva et al. (1994); (c) Bortolotti et al. (2002). (*) ICP-MS analyses; (°) ICP analyses. Normalization values for REE ratios are from Sun and McDonough (1989).

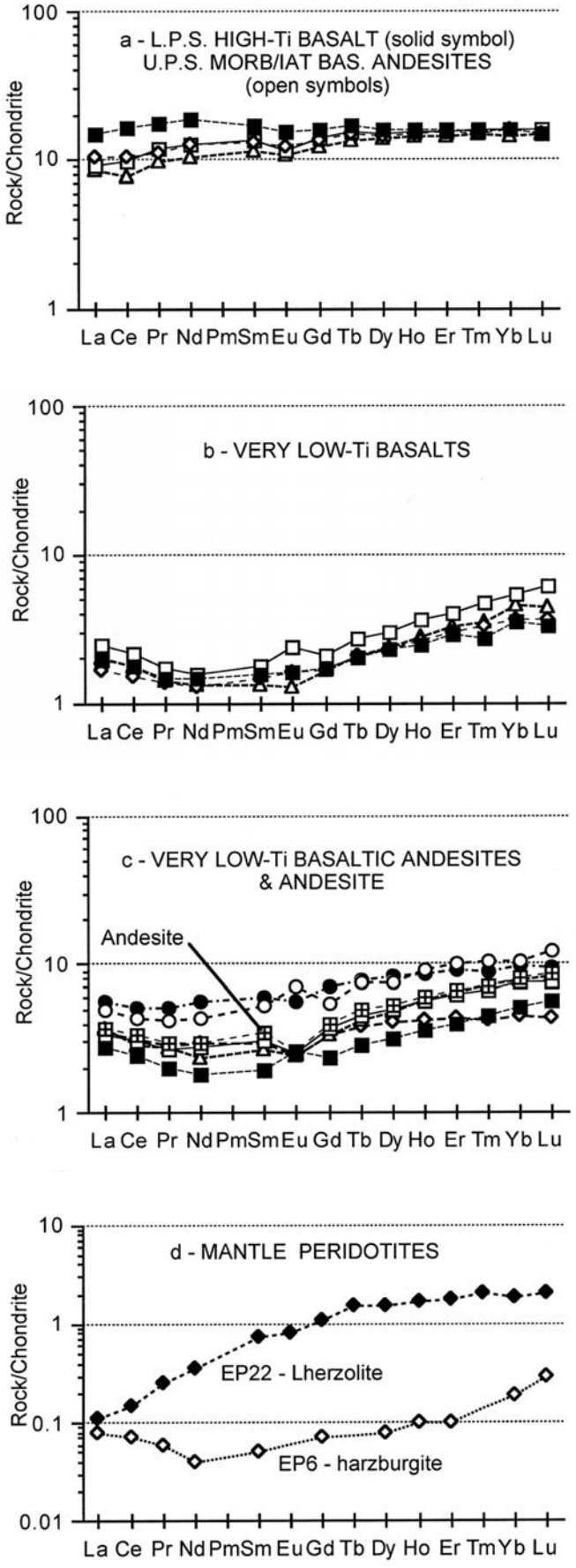

Fig. 6 - Chondrite-normalized (Sun and McDonough, 1989) REE patterns for volcanic and subvolcanic rocks from the Pindos Aspropotamos Complex (a, b, c) and mantle harzburgites from the Pindos Dramala Complex (d). Modified from Saccani and Photiades (2004).

1.9) in comparison with those of the lower pillow sequence (Table 3). Moreover, in spite of their more evolved nature, they display lower HFSE concentrations with flat patterns at 0.5-1 times N-MORB (Saccani and Photiades, 2004). These rocks show HREE concentrations (Fig. 6a) similar to those of basalts from the lower pillow sequence, but have comparatively greater LREE depletion (La_N/Sm_N = 0.68-0.80). In summary, basaltic rocks from the upper pillow sequence show overall geochemical characteristics which are intermediate between N-MORB and IAT compositions.

Dykes and massive lava flows interlayered in the pillow lavas are represented by very low-Ti basalts and basaltic andesites (Table 3), characterized by very low contents of HFSE (e.g., TiO_2 0.14-0.39%, P_2O_5, <0.01%, Zr 10-38 ppm, Y 7-16 ppm), between 0.1 and 1 times N-MORB composition (Saccani and Photiades, 2004). They display REE with the U-shaped patterns (Figs.6b, c) typical of boninites observed in forearc regions (Crawford et al., 1989; Falloon and Crawford, 1991), as well as in many ophiolitic complexes (e.g., Beccaluva and Serri, 1988; Bédard, 1999).

Mantle peridotites of the Dramala Complex (Upper Ophiolitic Unit) show compositional variations mainly reflected in their TiO_2, Al_2O_3, and CaO contents, as well as REE distributions (Table 3) related, in turn, to clinopyroxene abundance. The refractory and clinopyroxene-poor harzburgite (EP6) is characterized by low TiO_2, Al_2O_3 and CaO contents coupled with very depleted REE patterns (Fig. 6d). By contrast, the clinopyroxene-bearing harzburgites/lherzolite EP22 displays comparatively higher TiO_2 Al_2O_3 and CaO contents, as well as overall abundance of REE (Fig. 6d).

VOURINOS OPHIOLITES

Geological framework

The Vourinos Complex is located eastward of the Pindos Complex (Fig. 1a), and is thought to be continuous with the latter below the Meso-Hellenic through molasse (Ross and Zimmerman, 1996). This ophiolitic complex is largely dominated by mantle tectonites (Fig. 1d), consisting of massive harzburgite and deformed pods and lenses of dunite and chromitite. Mantle tectonites are frequently cross-cut by dunite and pyroxenite dykes, and overlain by ultramafic cumulates, mainly represented by dunite and subordinate chromitite and wehrlite. The generalized stratigraphic sequence of the Vourinos Complex (Fig. 2) continues upward with mafic cumulates, in which gabbronorites (with scarce ol-clinopyroxenite layers) predominate. Locally, mafic cumulates are topped by isotropic diorites and plagiogranites, as well as by magmatic breccias in the upper part of cumulate section. Dykes and sills of basaltic to dacitic compositions are found at the top of the diorites in the Krapa series, and are overlain by basaltic and andesitic massive lavas (Beccaluva et al., 1984). The ophiolitic sequence is topped by latest Bajocian-early Callovian radiolarian cherts (Chiari et al., 2003) followed by Albian-Aptian calcareous arenites and Cenomanian limestones. Sub-ophiolitic mélange and amphibolitic soles, dated as 171±4 Ma (Spray and Roddick, 1980), crop out in the eastern border of the massif (Fig. 1d). In the Rhodiani area (Fig. 1d) the Vourinos Complex is dismembered in several thrust sheets emplaced over the Pelagonian platform. These include an ultramafic unit, a volcanic unit, and a Middle-Late Jurassic carbonate platform sliver

Table 3 - Bulk-rock major and trace element analyses of selected volcanic, subvolcanic, and peridotitic rocks from the Pindos Ophiolites.

	ASPROPOTAMOS RIVER COMPLEX														DRAMALA COMPLEX	
	MORB LPS	MORB/IAT UPS			VERY LOW-Ti LAVAS AND DYKES										PERIDOTITES	
Sample	EP45	EP49	EP50	EP48	EP43	EP54	EP32	EP39	EP15	EP42	EP46	EP47	EP40	EP38	EP6	EP22
Rock	Bas	B.And	B.And	B.And	Bas	Bas	Bas	Bas	B.And	B.And	B.And	B.And	B.And	B.And	Harz	Lherz
Note	Pillow	Pillow	Dyke	Pillow	MLF	Dyke	Dyke	Dyke	MLF	Dyke	MLF	MLF	Dyke	Dyke		
XRF analyses:																
SiO_2	47.50	52.75	52.05	55.34	50.08	50.66	50.88	52.86	53.41	53.65	54.85	54.90	55.05	56.04	42.86	41.13
TiO_2	1.25	1.12	1.01	1.21	0.16	0.14	0.15	0.16	0.27	0.19	0.39	0.22	0.27	0.28	0.01	0.06
Al_2O_3	16.78	16.75	18.36	14.91	13.99	11.90	10.29	10.06	14.94	15.08	16.28	15.56	16.09	14.75	0.35	2.40
Fe_2O_3	1.15	1.33	1.25	1.42	1.08	1.13	1.10	1.06	0.81	1.15	1.25	1.20	1.16	1.34		
FeO	7.65	8.84	8.30	9.43	7.21	7.56	7.32	7.09	5.38	7.64	8.32	8.02	7.73	8.91	6.78	6.50
MnO	0.16	0.18	0.18	0.17	0.16	0.15	0.16	0.15	0.14	0.15	0.16	0.15	0.15	0.16	0.13	0.13
MgO	9.57	5.36	5.57	7.59	14.35	16.24	18.69	16.94	13.17	7.55	6.52	7.47	7.31	7.23	44.28	40.50
CaO	10.95	3.95	3.08	2.23	7.24	6.86	8.12	8.89	3.64	9.68	6.16	7.39	5.67	8.24	0.56	2.23
Na_2O	2.87	5.08	8.23	3.72	1.99	2.41	0.68	0.86	4.28	2.74	3.53	2.42	4.30	1.75	0.00	0.00
K_2O	0.06	2.28	0.12	1.31	0.10	0.20	0.08	0.03	0.03	0.01	0.57	0.19	0.23	0.04	0.00	0.00
P_2O_5	0.09	0.07	0.08	0.10	0.00	0.00	0.00	0.00	0.00	0.00	0.01	0.00	0.00	0.00	0.00	0.00
L.O.I.	1.96	2.29	1.77	2.56	3.64	2.75	2.53	1.89	3.93	2.16	1.96	2.48	2.03	1.27	5.03	7.04
Total	100.00	100.00	100.00	100.00	100.00	100.00	100.00	100.00	100.00	100.00	100.00	100.00	100.00	100.00	100.00	100.00
mg#	69.3	52.2	54.7	59.2	78.0	79.3	82.0	81.0	81.4	63.8	58.3	62.4	62.8	59.1	92.1	91.7
Pb	31	25	6	27	5	7	5	3	5	5	33	33	6	2	n.d.	7
Zn	78	79	69	89	77	54	61	64	61	65	69	76	71	64	42	42
Ni	140	11	11	12	187	268	310	228	53	56	24	76	52	42	2367	1934
Co	39	23	24	30	42	51	52	49	32	29	36	39	35	37	115	96
Cr	399	19	18	16	658	1105	1348	1082	111	74	47	138	111	72	2625	2580
V	247	307	255	314	264	233	231	212	173	290	243	263	249	299	31	70
Rb	5	42	n.d.	21	n.d.	3	2	n.d.	n.d.	n.d.	10	4	2	n.d.	n.d.	n.d.
Sr	155	139	122	107	82	52	29	41	49	126	125	111	107	88	n.d.	24
Ba	22	131	18	113	22	21	17	8	9	9	39	30	13	10	n.d.	6
Zr	107	67	54	68	12	10	11	11	30	14	38	17	22	23	n.d.	n.d.
ICP-MS analyses:																
Sc	31.7	29.6	27.3	29.1	47.5	27.8	24.7	31.6	128	42.4	23.1	37.9	28.3	34.9	5.16	8.64
Y	28.4	21.8	21.0	26.8	6.68	5.35	4.19	4.94	7.44	6.12	15.3	8.09	8.71	10.3	0.08	2.12
La	3.52	2.11	1.99	2.41	0.59	0.48	0.47	0.40	0.82	0.66	1.33	0.88	1.16	0.80	0.02	0.03
Ce	9.93	5.85	4.71	6.23	1.34	1.10	1.08	0.91	1.92	1.48	3.14	1.76	2.68	1.83	0.04	0.09
Pr	1.65	1.12	0.92	1.05	0.17	0.13	0.14	0.13	0.27	0.19	0.48	0.26	0.40	0.25	0.01	0.02
Nd	8.55	5.91	4.85	5.77	0.73	0.61	0.68	0.60	1.36	0.84	2.63	1.10	2.05	1.29	0.02	0.17
Sm	2.56	2.02	1.72	1.95	0.27	0.20	0.24	0.23	0.46	0.30	0.92	0.40	0.80	0.47	0.01	0.12
Eu	0.88	0.65	0.62	0.70	0.14	0.07	0.09	0.09	0.14	0.15	0.33	0.14	0.41	0.15	n.d.	0.05
Gd	3.28	2.80	2.48	2.77	0.43	0.34	0.36	0.35	0.70	0.48	1.46	0.70	1.11	0.75	0.01	0.22
Tb	0.62	0.56	0.51	0.55	0.10	0.08	0.08	0.08	0.14	0.11	0.30	0.16	0.29	0.17	n.d.	0.06
Dy	3.98	3.80	3.46	3.67	0.77	0.61	0.58	0.59	1.02	0.79	2.10	1.24	1.91	1.26	0.02	0.38
Ho	0.88	0.85	0.80	0.83	0.21	0.16	0.14	0.15	0.24	0.20	0.49	0.33	0.51	0.32	0.01	0.10
Er	2.62	2.55	2.39	2.52	0.67	0.55	0.48	0.49	0.72	0.66	1.50	1.05	1.67	1.03	0.02	0.30
Tm	0.38	0.40	0.37	0.38	0.12	0.09	0.07	0.08	0.11	0.11	0.23	0.18	0.26	0.17	n.d.	0.05
Yb	2.64	2.65	2.43	2.65	0.91	0.77	0.60	0.62	0.77	0.87	1.66	1.32	1.81	1.28	0.03	0.32
Lu	0.38	0.40	0.37	0.38	0.16	0.11	0.08	0.09	0.11	0.14	0.24	0.21	0.31	0.19	0.01	0.05
Nb	3.64	2.35	1.33	2.47	0.94	0.76	0.70	0.42	1.96	1.00	1.04	1.17	1.03	0.95	0.42	0.06
Hf	2.61	2.36	1.58	2.02	0.52	0.27	0.26	0.27	n.d.	0.63	1.01	0.53	0.96	0.57	0.02	0.09
Ta	0.25	0.16	0.09	0.17	0.10	0.08	0.17	0.05	0.14	0.16	0.09	0.11	0.25	0.07	0.47	0.06
Th	0.23	0.25	0.18	0.27	0.20	0.17	0.14	0.13	0.21	0.19	0.28	0.24	0.43	0.33	0.01	0.01
U	0.07	0.12	0.16	0.13	0.09	0.07	0.07	0.07	0.08	0.09	0.15	0.12	0.33	0.14	n.d.	n.d.
Ti/V	30	22		23	4	4	4	5	9	4	10	5	7	6		
Zr/Y	3.7	2.9	2.3	2.6	1.5	1.5	1.9	1.6	3.0	1.9	2.4	1.8	1.9	1.7		
Ti/Cr	19	360		453	1	1	1	1	15	15	51	10	15	24		
$(La/Sm)_N$	0.89	0.68	0.75	0.80	1.38	1.53	1.27	1.14	1.16	1.42	0.94	1.41	0.94	1.10	1.67	0.14
$(Sm/Yb)_N$	1.08	0.85	0.79	0.82	0.34	0.29	0.44	0.40	0.66	0.38	0.62	0.34	0.49	0.41	0.25	0.40
$(La/Yb)_N$	0.96	0.57	0.59	0.65	0.47	0.45	0.56	0.46	0.77	0.54	0.58	0.48	0.46	0.45	0.42	0.06

Abbreviations: LPS = lower pillow series; UPS = upper pillow series; Bas = basalt; B.And = basaltic andesite; Harz = harzburgite; Lherz = lherzolite; MLF = massive lava flow; mg# = molar Mg/(Mg+Fe)*100; n.d. = not detected. Data from Saccani and Photiades (2004). Normalization values for REE ratios are from Sun and McDonough (1989).

overlain by neritic to pelagic Cretaceous limestone (Photiades and Pomoni-Papaioannou, 2001; Carras et al., 2004).

Beccaluva et al. (1984) distinguished two differing magmatic series in the Vourinos Complex: (1) a predominant island-arc tholeiitic series represented by the Krapa Hills sequence, which includes wehrlites, clinopyroxenites, and gabbronorites, covered by volcanic and subvolcanic rocks; and (2) a subordinate and younger boninitic series represented by the Asprokambo dykes and associated websterites, layered gabbronorites, quartz-diorites, and granophyres.

Geochemistry

According to Beccaluva et al. (1984) the two volcanic and subvolcanic sequences of the Vourinos Complex consist of: (1) basalts, basaltic andesites, andesites, and dacites in the low-Ti series of the Krapa Hills; and (2) basalts, basaltic andesites, andesites, dacites, and rhyolites in the very low-Ti series of the Asprokambo (Table 4). Basaltic rocks from these groups can be readily distinguished on the basis of their Ti/V ratios (Fig. 3), which lie between 10 and 20 and less than 10 for the Krapa and Asprokambo series, respectively.

The Krapa basalts have Ti/Zr ratios (100-135) and Zr/Y ratios (2-2.6) typical of island arc tholeiites (Beccaluva et al. 1979), whereas the Asprokambo basaltic dykes show comparatively lower Ti/Zr (79-99), Zr/Y (1.8-2.2) and Al_2O_3/TiO_2 (33-77) ratios with affinities with boninitic rocks from western Pacific island arcs (Beccaluva and Serri, 1988). The Krapa and Asprokambo series are characterized by distinct crystallization orders, which are respectively: olivine - clinopyroxene - plagioclase - orthopyroxene – Fe-Ti-oxides, and (olivine) - orthopyroxene + clinopyroxene - plagioclase – amphibole. In addition, the early appearance of orthopyroxene, the presence of quartz - albite myrmekite in basaltic andesites and quartz phenocrysts in dacites from Asprokambo suggest a more saturated character of this series with respect to the Krapa series.

Moreover, the Krapa rocks are richer in TiO_2, Al_2O_3, FeO, and HFSE and are poorer in Ni and Cr with respect to the Asprokambo lavas (Table 4). Krapa basaltic rocks display LREE depleted patterns with overall REE concentrations from 5 to 10 times chondrite (Fig. 7a).

The most striking characteristics of the Asprokambo basaltic rocks are their extremely low contents of HFSE (TiO_2 0.19-0.44%, P_2O_5 0.01-0.02%, Zr 16-31 ppm, Y 9-15 ppm), associated with a relatively low Al_2O_3 (13.6-15.7%) and marked REE depletion. Their REE abundances range from 2 to 8 times chondrites (Fig. 7b). All these features coherently indicate similarities between the Asprokambo series and boninitic lavas found in the forearc regions of oceanic island arcs (Beccaluva and Serri, 1988; Crawford et al., 1989; Falloon and Crawford, 1991).

MAGMA GENESIS AND MANTLE SOURCES

From the data presented above, it results that four main groups of parental basic magmas occur in the Albanide-Hellenide ophiolites: (1) high-Ti basalts comparable to N-MORB; (2) low-Ti basalt-basaltic andesite,which are best equated to IAT; (3) basalts and basaltic andesites showing geochemical features intermediate between MORB and IAT; (4) very low-Ti basalt-basaltic andesite-andesite, resembling a boninite suite. The compositional differences between these magma types could be primarily related to different source characteristics that are associated, in turn, to distinct tectono-magmatic settings of formation. Moreover, the particular association of MORB, intermediate MORB/IAT, and boninitic rocks observed along some Mirdita volcanic sequences (e.g. the Kalur sequence, Bortolotti et al., 2002) and in the Pindos Aspropotamos Complex (Capedri et al., 1980; Saccani and Photiades, 2004) suggests that distinct magma sources were closely associated in space and time during the oceanic accretionary processes.

The overall REE and HFSE contents are commonly considered a distinctive geochemical characteristic of magma types and their related mantle sources, with particular regard to the degree of depletion(s) (Pearce et al., 1984, Pearce, 2003).

The high-Ti basalts corresponding to N-MORB composition (Figs. 4a and 6a) show the highest REE patterns and therefore represent magmas generated from the least depleted mantle sources.

The MORB/IAT intermediate basalts show relatively low REE concentrations (Fig. 4b) suggesting that they originated by partial melting of mantle sources that were more refractory with respect to MORB. Similar REE patterns can be observed in many SSZ basalts (Yumul, 1996; Klein and Karsten, 1995), and are considered the product of H_2O-assisted re-melting of a SSZ mantle wedge that already underwent MORB extraction. In fact, the marked LREE depletion (Figs.4b) of these basalts (La_N/Sm_N = 0.13-0.28) suggests that the SSZ mantle wedge did not undergo any significant enrichment by subduction-related fluids, except water. On the other hand, low-Ti and very low-Ti basaltic rocks, corre-

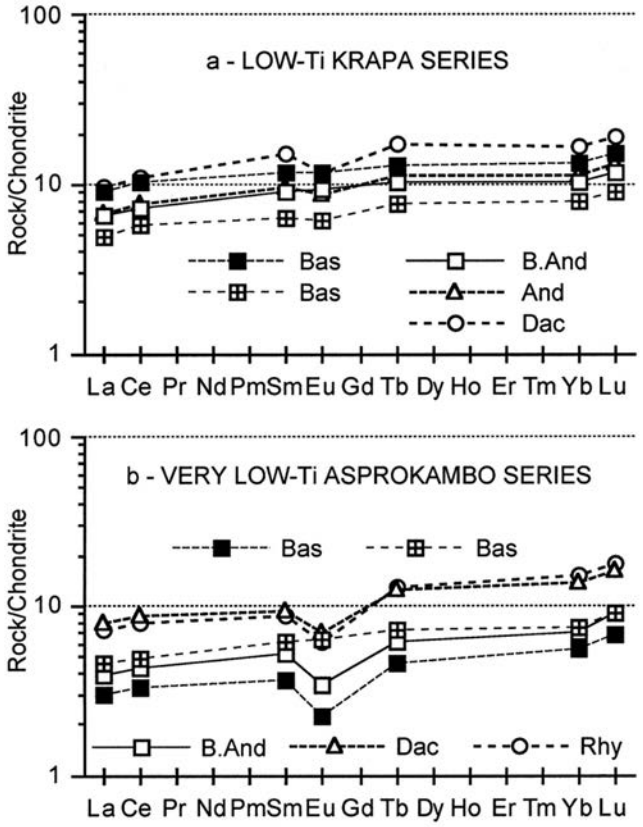

Fig. 7 - Chondrite-normalized (Sun and McDonough, 1989) REE patterns for volcanic and subvolcanic rocks from the Vourinos Ophiolites. a: low-Ti rocks from the Krapa series; b: - very low-Ti rocks from the Asprokambo series.

Table 4 - Bulk-rock major and trace element analyses of selected volcanic, and subvolcanic rocks from the Vourinos Ophiolites.

	KRAPA SERIES IAT					ASPROKAMBO SERIES VERY LOW-Ti				
Sample	AP-10-6	AP-26-7	AP-19-7	AP-9-6	AP-1-7	AP-3-4	AP-13-1	AP-1-3	AP-1-1	AP-5-1
Rock	Bas	Bas	B.And	And	Dac	Bas	Bas	B.And	Dac	Rhy
SiO_2	48.92	52.41	53.24	58.50	64.25	51.85	52.51	55.70	68.39	72.40
TiO_2	1.01	0.45	0.66	0.78	0.73	0.44	0.21	0.19	0.32	0.25
Al_2O_3	18.42	15.80	16.57	15.12	13.83	14.35	15.70	14.62	12.90	10.90
Fe_2O_3	1.47	1.07	1.21	1.23	1.03	1.02	0.91	0.83	0.77	0.65
FeO	9.80	7.16	8.10	8.23	6.86	6.79	6.05	5.56	5.14	4.30
MnO	n.a.	n.a.	n.a.	n.a.	n.a.	n.a.	n.a.	n.a.	n.a.	n.a.
MgO	4.12	8.10	5.23	4.55	2.63	6.75	8.20	5.86	1.72	1.45
CaO	8.15	4.35	2.95	2.86	1.22	12.06	8.80	9.55	2.60	3.10
Na_2O	3.85	3.56	4.85	4.41	5.02	1.21	2.56	2.54	4.18	3.51
K_2O	0.33	1.54	1.23	0.37	0.16		0.30	0.15	0.12	0.03
P_2O_5	0.06	0.02	0.03	0.05	0.07	0.02	0.01	0.01	0.03	0.04
L.O.I.	1.78	4.91	5.02	3.16	2.64	3.66	3.43	3.32	2.06	1.75
Total	97.9	99.4	99.1	99.3	98.4	98.2	98.7	98.3	98.2	98.4
mg#	43.1	67.1	53.8	49.9	40.8	64.1	70.9	65.5	37.6	37.8
Zn	82	101	97	80	96	63	74	94	78	64
Ni	30	47	33	27	20	105	86	57	31	15
Co	47	39	37	34	14	44	43	40	25	16
Cr	28	130	54	62	52	402	311	154	92	81
V	443	241	294	300	177	278	290	215	93	24
Rb	7	11	13	5	n.d.	3	5	6	5	n.d.
Sr	125	87	72	74	36	133	89	59	78	73
Nb	3	<2	<2	3	4	<2	<2	<2	3	4
Zr	58	27	35	47	66	27	16	24	35	37
Y	24	11	16	20	32	13	9	11	24	25
Sc	36.9	35.5	30.8	32.7	25.8	41.4	45.5	44.4	21.6	19.4
La	2.13	1.17	1.53	1.60	2.28	1.09	0.70	0.91	1.86	1.71
Ce	6.21	3.51	4.46	4.78	6.80	3.02	2.01	2.58	5.40	4.86
Sm	1.81	0.98	1.40	1.50	2.36	0.95	0.56	0.80	1.43	1.32
Eu	0.69	0.35	0.54	0.50	0.69	0.37	0.13	0.20	0.4	0.35
Tb	0.49	0.29	0.39	0.43	0.65	0.27	0.17	0.23	0.47	0.48
Yb	2.28	1.34	1.75	1.95	2.82	1.25	0.93	1.20	2.38	2.55
Lu	0.39	0.23	0.30	0.34	0.48	0.23	0.17	0.23	0.41	0.45
Hf	1.57	0.81	1.04	1.36	1.88	0.79	0.60	0.99	1.29	1.16
Ti/V	14	11	13	16		9	4	5		
Zr/Y	2.4	2.5	2.2	2.4	2.1	2.1	1.8	2.2	1.5	1.5
Ti/Cr	216	21	73	75		7	4	7		
$(La/Sm)_N$	0.76	0.77	0.71	0.69	0.62	0.74	0.81	0.73	0.84	0.84
$(Sm/Yb)_N$	0.88	0.81	0.89	0.85	0.93	0.84	0.67	0.74	0.67	0.58
$(La/Yb)_N$	0.67	0.63	0.63	0.59	0.58	0.63	0.54	0.54	0.56	0.48

Abbreviations: Bas = basalt; B.And = basaltic andesite; And = andesite; Dac = dacite; Rhy = rhyolite; mg# = molar Mg/(Mg+Fe)*100; n.d. = not detected; n.a. = not analyzed. Major and trace element analyses (except REE) are from Beccaluva et al. (1984). REE determined by ICP analyses. Normalization values for REE ratios are from Sun and McDonough (1989).

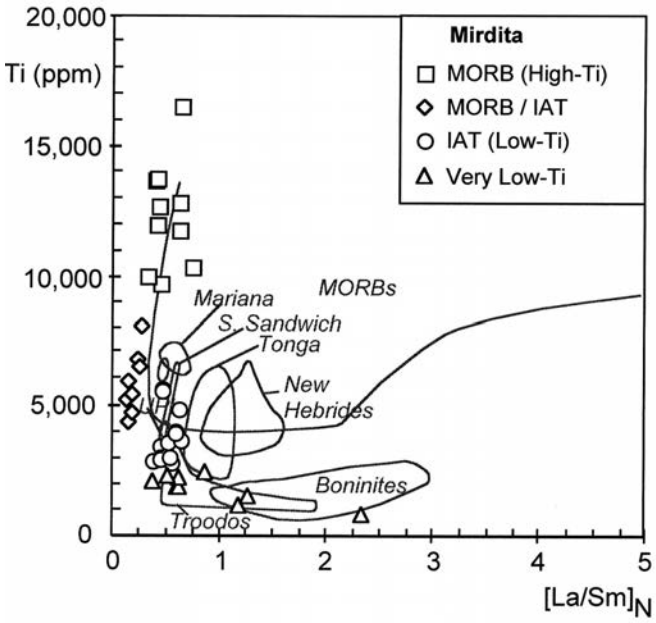

Fig. 8 - Ti vs. $(La/Sm)_N$ diagram for mafic volcanic and subvolcanic rocks from the Mirdita ophiolites (simplified after Beccaluva and Serri, 1988). MORBs and boninites from various localities, boninites from Troodos, as well as IAT data for New Hebrides, Tonga, South Sandwich, Mariana forearc, and Troodos upper pillow lavas (UPL) are reported for comparison (see Beccaluva and Serri, 1988 for references).

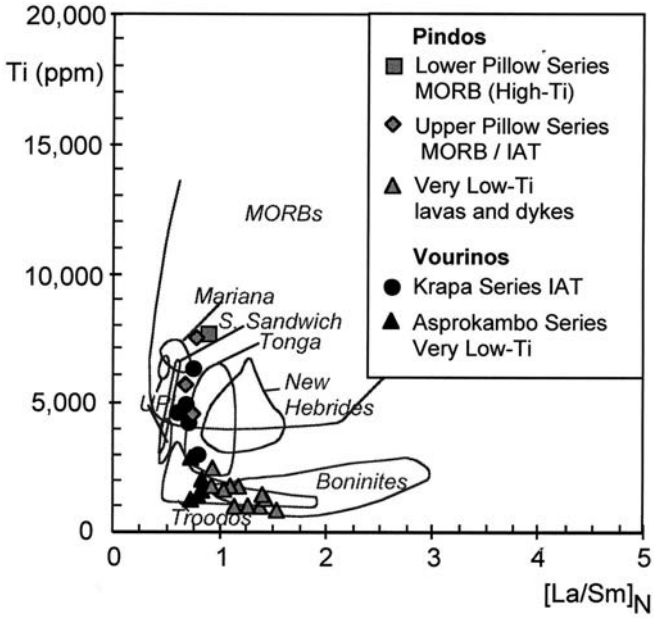

Fig. 9 - Ti vs. $(La/Sm)_N$ diagram for mafic volcanic and subvolcanic rocks from the Pindos and Vourinos ophiolites (simplified after Beccaluva and Serri, 1988). MORBs and boninites from various localities, boninites from Troodos, as well as IAT data for New Hebrides, Tonga, South Sandwich, Mariana forearc, and Troodos upper pillow lavas (UPL) are reported for comparison (see Beccaluva and Serri, 1988 for references).

sponding to IAT and boninites respectively, show more pronounced HREE and HFSE overall depletion coupled with variable LREE enrichment when compared with MORB/IAT intermediate basalts (Figs.5, 6b,c, 7). This is usually interpreted as resulting from partial melting of progressively more refractory mantle sources variably enriched in the most incompatible elements (LREE and LFSE) from subduction-derived hydrous fluids.

Similarly, as suggested by Beccaluva and Serri (1988), the gradual Ti decrease and $(La/Sm)_N$ increase observed from MORB to IAT and Boninites (Figs.8, 9) are compatible with high degrees of melting of progressively more refractory mantle sources under variable hydrous conditions which are also responsible for the LREE enrichment from the subduction zone.

An estimate of the degree of depletion of the mantle source(s) can be made by plotting a compatible versus an incompatible element, such as Cr and Y (Pearce, 1983). This projection depicts both the possible mantle sources and the degree of partial melting for the different magmas. Three possible mantle sources generated by incremental batch melting of a MOR-type source (Murton, 1989), are reported in Fig. 10 for the genesis of MOR, IAT, and boninitic rocks, respectively. M1 corresponds to an undepleted asthenospheric (MORB) source, whereas M2 corresponds to a lherzolitic mantle source that experienced about 20% MORB extraction and M3 represents a harzburgitic source residual after about further 12% melt extraction from source M2. According to this model, MORBs from Albanide-Hellenide ophiolites are compatible with about 10 to 20% partial melting of source M1; MORB/IAT intermediate basalts, and IATs may represent 8-10% and 10-20 % partial melting of source M2, respectively. It should be noted that degrees of melting exceeding 30% would require exceptionally hot and/or wet melting regimes starting from less depleted mantle sources (Tatsumi and Eggins, 1995).

From the above, it is evident that sources M2 (lherzolitic) and M3 (harzburgitic) correspond to refractory mantle residua after extraction of MORB and IAT magmas, respectively. It should also be noted that, in the Albanide-Hellenide system, mantle lherzolites are associated with high-Ti ophiolites (Western Belt) whereas mantle harzburgites typically belong to the SSZ ophiolites (Eastern Belt).

The REE distribution of basaltic rocks and associated mantle lithologies from the Albanide-Hellenide ophiolites may be used to put further constraints on mutual relationships between melt, source and refractory residuum (Figs.11, 12). The generation of MORB/IAT intermediate basalts (e.g. RU200 and RU274) can be accounted for by about 10% partial melting of the Pindos Cpx-poor lherzolite EP22 (Fig. 11), which is compositionally similar to source M2. The very low-Ti boninitic rocks (AL130, EP42, EP43 in Fig. 12) may result from 30% partial melting of the lherzolitic source S4, enriched in LREE by subduction-related fluids, as modelled by Beccaluva et al. (1984) for the Vourinos Ophiolites. This source is in excellent agreement with the middle to HREE pattern of the Cpx-poor lherzolite EP22. The calculated residuum (R in Fig. 12) has a REE pattern very similar to the Pindos Cpx-free harzburgite EP6 (Fig. 12). It may be concluded that boninitic magmas are most likely represent high degree of partial melting of Cpx-poor lherzolites to Cpx-rich harzburgites variably modified by LREE- and LFSE-enriched hydrous fluids. The related refractory residua correspond to the highly depleted mantle harzburgites commonly observed in the Albanide-Hellenide Eastern Belt Ophiolites.

Experimental anhydrous melts obtained at various temperature, pressures, and degrees of melting by Hirose and Kushiro (1993) are plotted in the normative olivine-plagioclase-silica diagram of Fig. 13. The most primitive MORB samples from both Mirdita and Pindos ophiolites cluster close to the pseudo-invariant points between 10 and 15 kbar

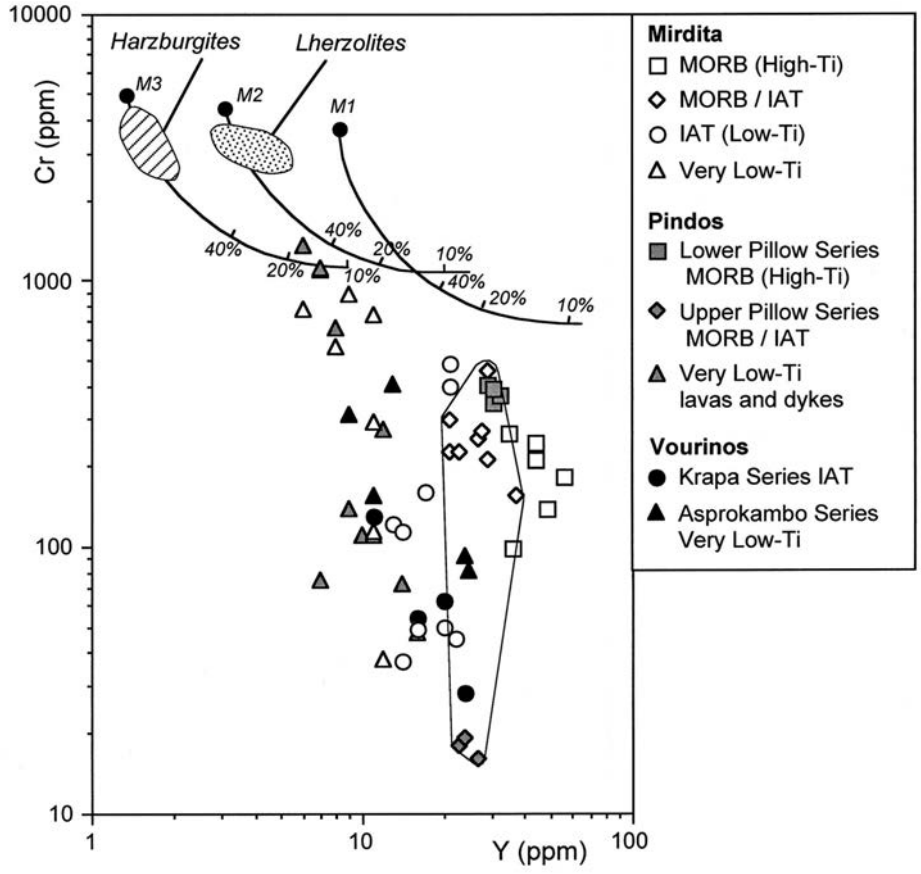

Fig. 10 - Cr vs. Y diagram (modified after Pearce, 1983) for mafic volcanic and subvolcanic rocks from the Mirdita, Pindos, and Vourinos ophiolites. Mantle source compositions and melting paths for incremental batch melting are from Murton (1989). M1: calculated MORB source; M2: residue after 20% MORB extraction; M3: residue after 12% melt extraction from M2. Field encircles MORB/IAT intermediate basalts from different localities. Compositional fields of harzburgites and lherzolites from Mirdita, Pindos, and Vourinos ophiolites are also reported (Montigny et al., 1973; Beccaluva et al., 1994; Saccani and Photiades, 2004). See text for explanation.

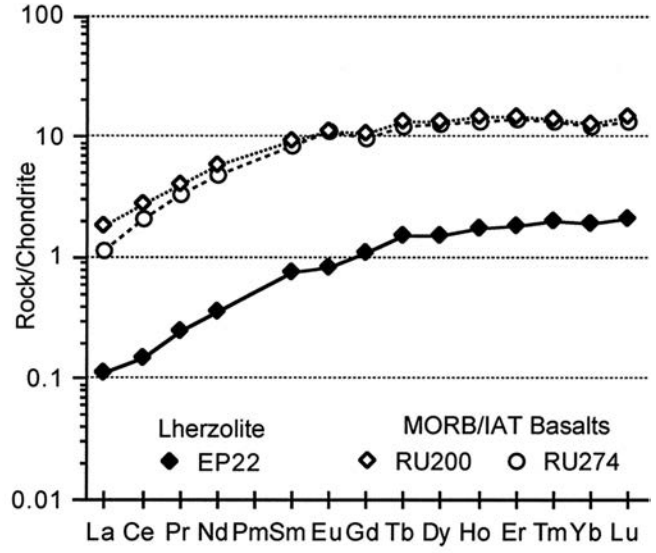

Fig. 11 - Chondrite-normalized (Sun and McDonough, 1989) REE patterns for Pindos lherzolite EP22 (Saccani and Photiades, 2004) and MORB/IAT intermediate basalts RU200 and RU274 from Mirdita Western Belt Ophiolites.

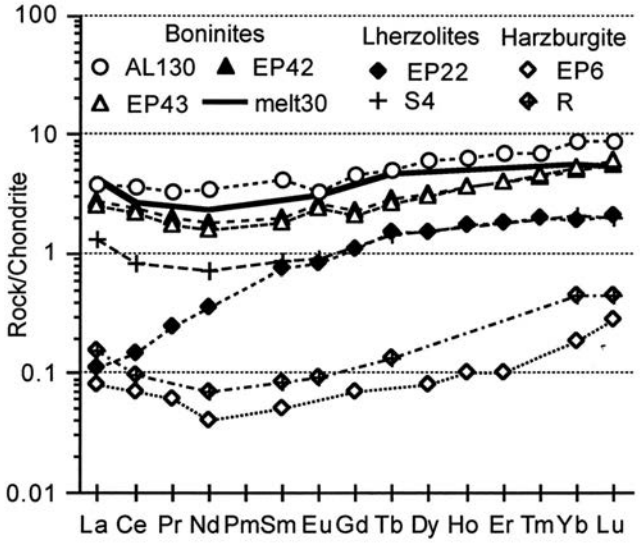

Fig. 12 - Chondrite-normalized (Sun and McDonough, 1989) REE patterns for Pindos harzburgite EP6 and very low-Ti basalts AL130 from Mirdita Eastern Belt Ophiolites and EP42, EP43 from Pindos ophiolites (data for Pindos samples are from Saccani and Photiades, 2004). The patterns of a melt (melt30) corresponding to 30% equilibrium partial melting of a hypothetical source (S4), and relative residuum (R), modelled according to Beccaluva et al. (1984), are also shown.

(Fig. 13), corresponding to 1300°C temperature - 30% partial melting and 1350°C - 28% partial melting, respectively.

Experimental melts obtained from a spinel lherzolite at 10 kbar under water undersaturated conditions (Hirose and Kawamoto, 1995), as well as compositional fields for Troodos andesites and dacites (Thy and Xenophontos, 1991) are reported in the normative olivine-plagioclase-silica diagram of Fig. 14. The primitive IAT basalts from Mirdita (Fig. 14a) correspond to experimental melts at about 18-30% partial melting at 10 kbar pressure. More evolved basalts, basaltic andesites, and andesites are multi-saturated in pyroxenes and plagioclase, while dacites and rhyolites approach quartz-saturated compositions (Fig. 14a). Similar results are observed for Mirdita boninitic very low-Ti basalts,

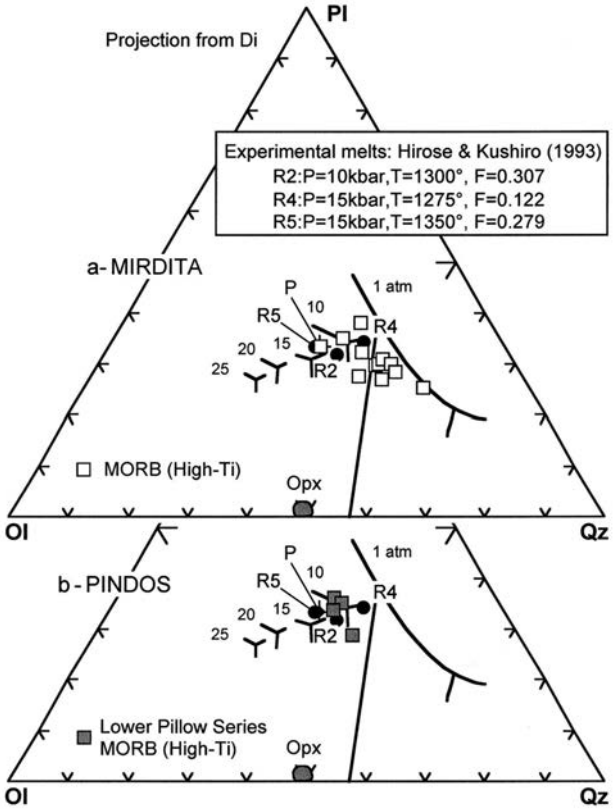

Fig. 13 - Pseudo-ternary diagram of normative plagioclase-olivine-silica (Pl, Ol, Qz) projected from diopside (Walker et al., 1979) for high-Ti volcanics from Mirdita Western Belt Ophiolites (a) and Pindos Ophiolites (b). Solid phase boundaries from experimental melts obtained from anhydrous conditions (Hirose and Kushiro, 1993) are also projected for comparison.

basaltic andesites, and andesites (Fig. 14b). Very low-Ti basalts from Pindos ophiolites (Fig. 14c) cluster around experimental melts at 29-38% partial melting. Basaltic andesites and andesites, in turn, plot along the 10 kbar pyroxene-plagioclase cotectic (Fig. 14c). Both low-Ti and very low-Ti rocks from Vourinos ophiolites (Fig. 14d) are plagioclase-2pyroxene multisaturated with the most evolved compositions reaching the quartz field.

TECTONO-MAGMATIC MODEL

The regional reconstruction of the Neo-Tethyan basin in the eastern Mediterranean implies (1) the opening of the Mirdita-Pindos oceanic basin between Adria (in the west) and Pelagonian (in the east) continental margins during the Late Triassic-Middle Jurassic (Jones and Robertson, 1991; Beccaluva et al., 1994; Robertson, 2002; Saccani et al., 2003, 2004), and (2) its closure by an intra-oceanic subduction during the Middle-Late Jurassic (Beccaluva et al., 1984; Beccaluva et al., 1994; Bortolotti et al., 2002; Robertson, 2002).

The discussion in this section is focused on the possible geodynamic setting(s) in which the different ophiolitic types formed.

Several models have been provided to explain the coexistence of MORB and SSZ ophiolites, as well as the tectono-magmatic significance of MORB-IAT intermediate basalts and their relationships with typical MORBs and boninites in the Albanide-Hellenide system. In fact, the occurrence of MORB/IAT basalts has been documented in volcanic sequences from the northern Mirdita (Bortolotti et al., 1996; 2002), southern Mirdita (Hoeck et al., 2002), Pindos (Saccani and Photiades, 2004) and Othrys Massifs (Photiades et al., 2003). MORB/IAT intermediate basalts are always in close spatial/temporal association with typical MOR- and other SSZ-type volcanics, indicating that distinctly different magma sources were contemporaneously active in a relatively restricted sector across the supra-subduction region (Bortolotti et al., 1996; 2002; Bébien et al., 2000; Hoeck et al., 2002).

According to the two-dimensional geophysical model proposed by Bébien et al. (2000) and Insergueix-Filippi et

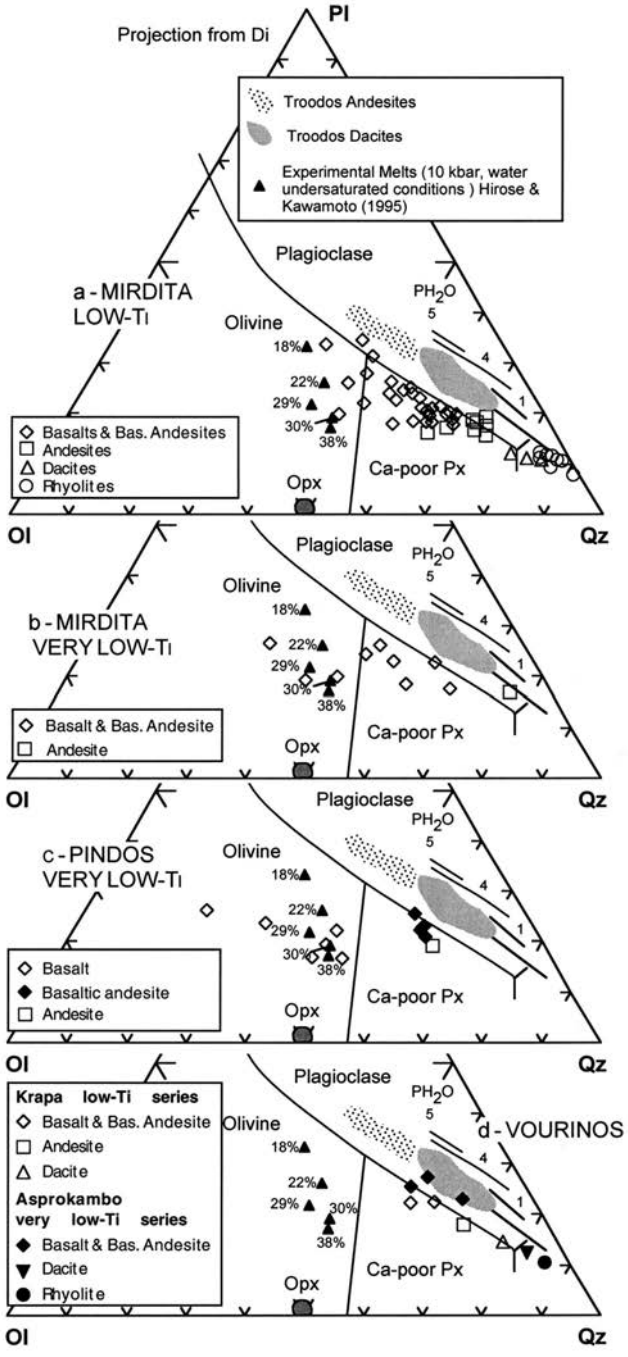

Fig. 14 - Pseudo-ternary diagram of normative plagioclase-olivine-silica (Pl, Ol, Qz) projected from diopside (Walker et al., 1979) for low-Ti and very low-Ti volcanics from Mirdita Eastern Belt (a, b), Pindos (c), and Vourinos (d) ophiolites. The effect of hydrated pressure on the plagioclase-augite-orthopyroxene is based on Merzbacher and Eggler (1984). Experimental melts obtained from water undersaturated conditions (Hirose and Kawamoto, 1995) and compositional fields for Troodos andesites and Dacites (Thy and Xenophontos, 1991) are also projected for comparison.

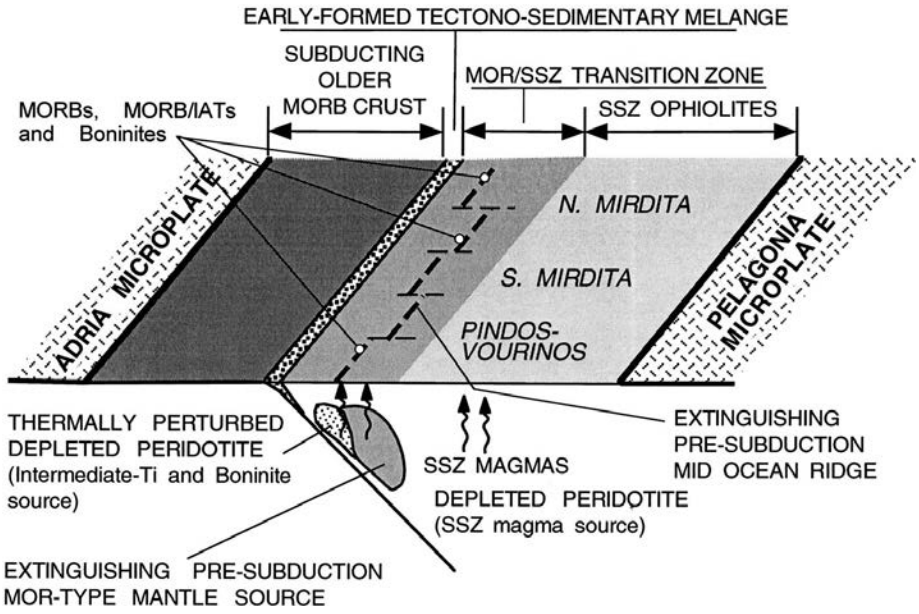

Fig. 15 - Schematic geodynamic model for formation of the Mirdita-Pindos-Vourinos ophiolites according to the model of subduction initiated in proximity of a former mid-ocean ridge (modified from Bébien et al., 2000; Bortolotti et al., 2002; Photiades et al., 2003). SSZ ophiolites include IAT and boninitic series. Tectonic-dominated mélange includes Triassic T-MORBs, N-MORBs, and WPBs, as well as Jurassic N-MORBs; sedimentary-dominated mélange includes Jurassic N-MORBs, MORB/IATs, and boninites (Photiades et al., 2003; Saccani et al., 2003; Saccani et al., 2004).

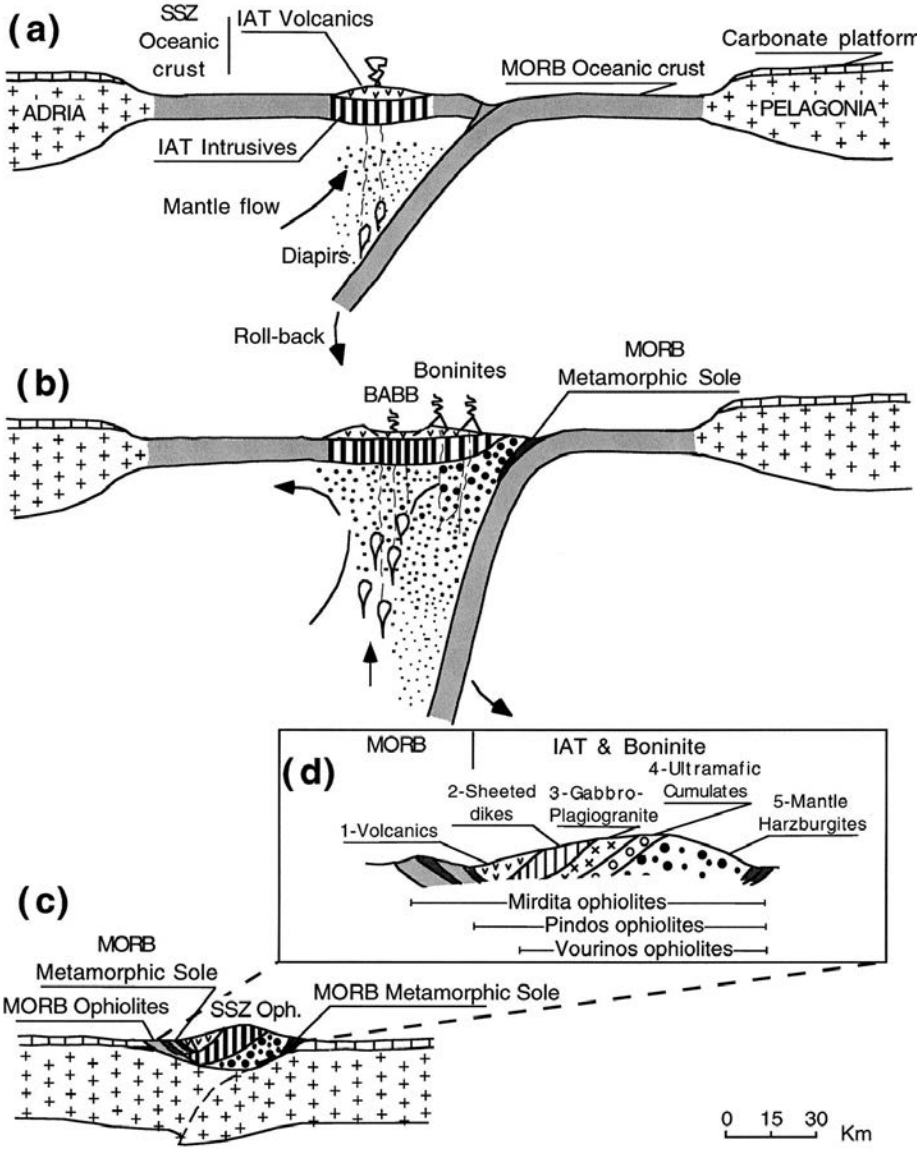

Fig. 16 - Sketch sections showing the development of SSZ oceanic lithosphere in the Albanide-Hellenide ophiolites. Modified after Beccaluva et al. (2004). Scale is approximate. See text for detailed explanation. (a) nascent arc generated by intra-oceanic subduction in a MORB oceanic basin with development of IAT magmatism from ascending mantle diapirs (lightly stippled). (b) continuous slab sinking and retreat, and generation of boninite magmatism by shallow partial melting of wedged wet mantle diapirs residual after IAT extraction (medium stippled), leaving residual depleted harzburgites (heavy stippled). (c) convergence processes and obduction onto the Pelagonian continental margin of large and relatively intact lithospheric sections of SSZ ophiolites. (d) generalized cross-section of the Albanide-Hellenide ophiolites referred to Mirdita, Pindos, and Vourinos ophiolitic complexes. Explanation: 1) basaltic to rhyodacitic pillowed and massive lavas volcanics, mostly with IAT (and minor boninitic) magmatic affinity; 2) large sheeted dike complexes with the same compositional range and affinity of volcanics, representing the temporary conduits from the underlying magma chambers (intrusives) to the eruptive system; 3) multiple intrusions consisting of cumulitic layered and isotropic gabbro-norite, with minor quartz-diorite and plagiogranite; 4) multiple intrusions of ultramafic cumulates consisting of dunite (plus chromitite), wehrlite, lherzolite, websterite, and clinopyroxenite; 5) mantle tectonites, mostly harzburgitic in composition, including dunite plus chromitite lenses. Pindos ophiolites also include relics of MORB crust not represented in this figure. Sections in (d) are compiled from Beccaluva et al. (1994), Jones et al. (1991), Beccaluva et al. (1984).

al. (2000), the possible tectono-magmatic setting in which Albanide-Hellenide ophiolites formed is an intra-oceanic, east-dipping subduction located near an active mid-ocean spreading ridge. In this model, Bortolotti et al. (2002) and Hoeck et al. (2002) suggested that MORB/IAT basalts were generated from partial melting of relatively hot, depleted peridotites in a supra-subduction mantle wedge, thermally perturbed by the nearby active mid-ocean ridge (Fig. 15). Accordingly, MORB magmas are produced in the active mid-ocean ridge whereas IAT and boninites of the Mirdita Eastern Belt and Vourinos represent a mature arc stage.

Hoeck et al. (2002) considered an alternative model, based on the comparison with the triangular-shaped present-day Lau Basin, suggesting that Albanide-Hellenide ophiolites formed by backarc spreading which was oblique with respect to a west-dipping subduction zone. As a consequence, subduction-related fluids could only influence the narrower sector of the backarc basin, producing MORB/IAT intermediate basalts.

Recently, Beccaluva et al. (2004) proposed a model that may explain the zonal arrangement of MORB and SSZ Tethyan ophiolites, as well as the multiple partial melting processes, which progressively affected sub-arc mantle sources. This model integrates both the tectono-magmatic evolution of western Pacific-type arc-backarc basin systems (Crawford et al., 1981, 1989; Beccaluva & Serri, 1988; Pearce et al., 1992; Pearce & Parkinson, 1993; Taylor & Natland eds., 1995; Gribble et al., 1998), and the mode of subduction, with particular regard to the steepening of the subducted slab, backarc opening and subduction retreat (Uyeda & Kanamori, 1979; Dewey, 1980).

For the Albanide-Hellenide ophiolites, the more appropriate model (Fig. 16) implies a low plate-convergence velocity, which allows an accentuated steepening and retreat of the subducting slab, accompanied by progressive decoupling of the converging plates and intense mantle diapirism and extension in the upper plate. Accordingly, the tectono-magmatic evolution of the Albanide-Hellenide ophiolites can be proposed as follows.

After the Triassic rifting stage, a MORB-type oceanic lithosphere formed between the Adria and Pelagonian continental blocks. Intra-oceanic subduction within the MORB-type lithosphere resulted in a SSZ basaltic magmatism with IAT affinity, and generation of a nascent arc mostly with low-Ti basaltic to andesitic volcanics and ultramafic to gabbro-noritic intrusives (Fig. 16a). Nearly open system conditions and continuous supply of undifferentiated basaltic magmas are suggested by the presence of widespread sheeted dike complexes, implying that the extension rate in the upper plate is progressively balanced by the roll-back and retreat of the subducted slab. The progressive slab sinking and retreat led to increasing asthenospheric diapirism from the arc axis to the forearc region, which caused shallow partial melting of the depleted sub-arc mantle with generation of boninites and/or very low-Ti tholeiites (Fig. 16b). Backarc basin basalts (BABB) with intermediate IAT/MORB characteristics, resulting from the interference of MORB-source mantle diapirs with suprasubduction mantle sources, may eventually have erupted at the spreading axis. As the interarc basin widens the spreading centres moved away from the converging margin, with subsequent decreasing influence of the subducted slab on magmas, which may reach pure MORB compositions. Diapiric ascent and wedging of highly depleted harzburgite-dunite mantle, residual after boninite extraction, occurs beneath the forearc region (Fig. 16b).

The convergence processes finally caused obduction onto the Pelagonian continental margin (often with an interposed metamorphic sole) of large and relatively intact lithospheric sections of SSZ ophiolites (Figs. 16c, d). This metamorphic sole has a MORB affinity, and is contemporaneous with, or slightly older than, the SSZ ophiolites. It thus represents relics of the pristine MORB lithosphere overthrust by the still hot ophiolitic slab. The subsequent tectonic evolution is characterized by back-thrusting onto the Adriatic margin during continental collision.

ACKNOWLEDGEMENTS

The authors are grateful to I. Premti, and A. Photiades for their precious help during field work and scientific discussions. Many thanks go to R. Tassinari for analytical facilities, as well as to J.A. Pearce and A. Photiades for their helpful reviews.

REFERENCES

Bébien J., Dubois R., Mercier J.L. and Vérgely P., 1984. Diversité du volcanisme dans les domaines les plus internes des Hellenides : l'Unité d'Aspro Vrissi (Macedonie greque). C.R. Acad. Sc. Paris, 298: 49-52.

Bébien J., Shallo M., Manika K. and Gega D., 1998. The Shebenik Massif (Albania): A link between MOR- and SSZ-type ophiolites? Ofioliti, 23: 7-15.

Bébien J., Dimo-Lahitte A., Vergély P., Insergueix-Filippi D. and Dupeyrat L., 2000. Albanian Ophiolites. I – magmatic and metamorphic processes associated with the initiation of a subduction. Ofioliti, 25: 47-53.

Beccaluva L., Ohnenstetter D. and Ohnenstetter M., 1979. Geochemical discrimination between ocean-floor and island-arc tholeiites-application to some ophiolites. Canadian Jour. Earth Sci., 16: 1874-1882.

Beccaluva L., Girolamo P.D., Macciotta G. and Morra V., 1983. Magma affinities and fractionation trends in ophiolites. Ofioliti, 8: 307-324.

Beccaluva L., Ohnenstetter D., Ohnenstetter M. and Paupy A., 1984. Two magmatic series with island arc affinities within the Vourinos ophiolite. Contrib. Mineral. Petrol., 85: 253-271.

Beccaluva L. and Serri G., 1988. Boninitic and low-Ti subduction-related lavas from intraoceanic arc-backarc systems and low-Ti ophiolites: a reappraisal of their petrogenesis and original tectonic setting. Tectonophysics, 146: 291-315.

Beccaluva L., Coltorti M., Premti I., Saccani E., Siena F. and Zeda. O., 1994. Mid-Ocean Ridge and Suprasubduction affinities in the Ophiolitic Belts from Albania. In: L. Beccaluva (Ed.), Albanian ophiolites: State of the art and perspectives. Ofioliti, 19: 77-96.

Beccaluva L., Shallo M., Coltorti M., Premti I. and Siena F., 1997. Albania. In: Moores E.M. and Fairbridge R.W. (Eds.) Encyclopedia of European and Asian Regional Geology. Chapman and Hall: 7-16.

Beccaluva L., Coltorti M., Giunta G. and Siena F., 2004. Tethyan vs Cordilleran ophiolites: A reappraisal of distinctive tectono-magmatic features of supra-subduction complexes in relation to the subduction mode. Tectonophysics (in press).

Bédard J.H., 1999. Petrogenesis of boninites from the Betts Cove Ophiolite, Newfoundland, Canada: Identification of subducted source components. Jour. Petrol., 40: 1853-1889

Bortolotti V., Kodra A., Marroni M., Mustafa F., Pandolfi L., Principi G. and Saccani E., 1996. Geology and petrology of ophiolitic sequences in the central Mirdita region (northern Albania). Ofioliti, 21: 3-20.

Bortolotti V., Marroni M., Pandolfi L., Principi G. and Saccani E., 2002. Interaction between mid-ocean ridge and subduction magmatism in Albanian ophiolites. J. Geol., 110: 561-576.

Capedri S., Venturelli G., Bocchi G., Dostal J., Garuti G. and Rossi A., 1980. The Geochemistry and Petrogenesis of an Ophiolitic Sequence from Pindos, Greece. Contrib. Mineral. Petrol., 74: 189-200.

Carosi R., Cortesogno L., Gaggero L., and Marroni M., 1996. Geological and petrological features of the metamorphic sole from the Mirdita ophiolites, northern Albania. Ofioliti, 21: 21-40.

Carras N., Fazzuoli M. and Photiades A., 2004. Transition from carbonate platform to pelagic deposition (Mid Jurassic-Late Cretaceous, Vourinos Massif, Northern Greece. Riv. It. Pal. Strat., 110: 345-355.

Chiari M., Bortolotti V., Marcucci M., Photiades A. and Principi G., 2003. The Middle Jurassic siliceous sedimentary cover of the top of the Vourinos ophiolite (Greece). Ofioliti, 28: 95-103.

Crawford A.J., Beccaluva L. and Serri G., 1981. Tectono-magmatic evolution of the West Philippine-Mariana region and the origin of boninites. Earth and Planet. Sci. Letters, 54: 346-356.

Crawford A.J., Falloon A. and Green D.H., 1989. Classification, petrogenesis and tectonic setting of boninites. In: A.J. Crawford (Editor), Boninites and related rocks. Unwin Hyman, London: 1-49.

Dewey J.F., 1980. Episodicity, sequence and style at convergent plate boundaries. In: D.W. Strangway (Ed.), The continental crust and its mineral deposits, Geol. Ass. Sp. Paper, 20: 553-573.

Grimble R.F., Stern R.J., Newman S., Bloomer S.H. and O'Heary T., 1998. Chemical and Isotopic Composition of lavas from the northern Mariana Trough: Implications for Magmagenesis in Back-arc Basins. Jour. Petrol., 39: 125-154.

Falloon T.J. and Crawford A.J., 1991. The petrogenesis of high-calcium boninite lavas dredged from the northern Tonga ridge. Earth Planet. Sci. Letters, 102: 375-394.

Franzini M., Leoni L. and Saitta M., 1972. A simple method to valuate the matrix effect in X-ray fluorescence analysis. X-Ray Spectrometry, 1: 151-154.

Hirose K. and Kushiro I., 1993. Partial melting of dry peridotites at high pressures: determination of compositions of melts segregated from peridotite using aggregates of diamond. Earth Planet. Sci. Letters, 114: 477-489.

Hirose K. and Kawamoto T., 1995. Hydrous partial melting of lherzolite at 1 GPa: The effect of H2O on the genesis of basaltic magmas. Earth Planet. Sci. Letters, 133: 463-473.

Hoeck V., Koller F., Meisel T., Onuzi K. and Kneringer E., 2002. The Jurassic South Albanian ophiolites: MOR- vs. SSZ-type ophiolites. Lithos, 65: 143-164.

Insergueix-Filippi D., Dupeyrat L., Dimo-Lahitte A., Vergely P. and Bébien J., 2000. Albanian ophiolites. II - Model of subduction zone infancy at a Mid-ocean ridge. Ofioliti, 25: 47-53.

Jones G. and Robertson A.H.F., 1991. Tectono-stratigraphic evolution of the Mesozoic Pindos ophiolite and related units, northwestern Greece. Jour. Geol. Soc. London, 148: 267-288.

Jones G., Robertson A.H.F. and Cann J.R., 1991. Genesis and emplacement of the supra-subduction zone Pindos ophiolite, northwestern Greece. Tj. Peters et al. (Eds), Ophiolite genesis and evolution of oceanic lithosphere, Ministry of Petroleum and Minerals, Sultanate of Oman: 771-799.

Kemp A.E.S. and McCaig A., 1984. Origin and significance of rocks in an imbricate thrust zone beneath the Pindos Ophiolite, northwestern Greece. In: A.H.F. Robertson and J.E. Dixon (Editors), The geological evolution of the eastern Mediterranean. Geol. Soc. London Sp. Publ., 17: 569-580.

Klein E.M. and Kastens J.L., 1995. Ocean-ridge basalts with convergent-margin geochemical affinities from the Chile Ridge. Nature, 374: 52-57.

Kostopoulos D., 1988. Geochemistry and tectonic setting of the Pindos Ophiolite, northwestern Greece. PhD thesis, University of Newcastle-upon-Tyne, 498 pp.

Marcucci M., Kodra A., Pirdeni A and Gjata T., 1994. Radiolarian assemblages in the Triassic and Jurassic cherts of Albania. In: L. Beccaluva (Ed.), Albanian ophiolites: State of the art and perspectives. Ofioliti, 19: 105-114.

Marcucci M., and Prela M., 1996. The Lumi i zi, (Puke) section of the Kalur Cherts: Radiolarian assemblages and comparison with other sections in northern Albania. Ofioliti, 21: 71-76.

Mavrides A., Kelepertzis A., Faugères L., Tsaila-Monopoli S., Mostler L. and Dimou E., 1982. Geological map of Greece, "SIATISTA sheet" in scale 1:50.000. Athens Institute of Geology and Mineral Exploration.

Mavrides A., Kelepertzis A., Tsaila-Monopoli S. and Skourtsis-Koroneou V., 1991. Geological map of Greece, "KNIDHI sheet" in scale 1:50.000. Athens Institute of Geology and Mineral Exploration.

Merzbacher C. and Eggler D.H., 1984. A magmatic geohygrometer: application to Mount St. Helens and other dacitic magmas. Geology, 12: 587-590.

Moores E.G., 1969. Petrology and structure of the Vourinos ophiolite complex of Northern Greece. Geol. Soc. Am. Sp. Paper, 118: 74pp.

Montigny R., Bougault H., Bottinga Y. and Allegre C.J., 1973. Trace element geochemistry and genesis of the Pindos ophiolite suite. Geochim. Cosmochim. Acta, 37: 2135-2147.

Murton B.J., 1989. Tectonic controls on boninite genesis. In: A.D. Saunders and M.J. Norry (Eds.), Magmatism in the Ocean Basins. Geol. Soc. London Sp. Publ., 42: 347-377.

Pearce J.A., 1983. Role of the Sub-continental Lithosphere in Magma Genesis at Active Continental Margin. In: C.J. Hawkesworth and M.J. Norry (Editors), Continental basalts and mantle xenoliths. Shiva, Nantwich: 230-249.

Pearce J.A., Lippard S.J. and Roberts S., 1984. Characteristics and tectonic significance of supra-subduction zone ophiolites. Geol. Soc.London Sp. Publ., 16: 77-94.

Pearce J.A., van der Laan S.R., Arculus R.J., Murton B.J., Ishii T., Peate D.W. and Parkinson I.J., 1992. Boninite and harzburgite from Leg 125 (Bonin-Mariana forearc): a case study of magma genesis during the initial stage of subduction. Proc. ODP, Sci. Results (P. Fryer, J.A. Pearce, L.B. Stokking et al., Eds.) 125, College Station, TX (Ocean Drilling Program): 623-659.

Pearce J.A. and Parkinson I.J., 1993. Trace element models for mantle melting: application to volcanic arc petrogenesis. In. H.M. Princiard, T. Alabaster, N.B.W. Harris and C.R. Neary (Eds.), Geol. Soc. London Sp. Publ., 76: 373-403.

Pearce J.A., 2003. Supra-subduction zone ophiolites: The search for modern analogues. In: Dilek Y. and Newcomb S. (Eds.), Ophiolite concept and the evolution of geological thought, Geol. Soc. Am. Sp. Paper, 373: 269-293.

Pe-Piper G. and Piper D.J.W., 2002. The igneous rocks of Greece. The anatomy of an orogen. Gebruder Borntraeger, Berlin: 573 p.

Photiades A. and Pomoni-Papaioannou F., 2001. Contribution to the structural study of the Rhodiani ophiolites, Vourinos Massif. Bull. Geol. Soc. Greece, XXXIV/1: 111-118.

Photiades A., Saccani E. and Tassinari R., 2003. Petrogenesis and tectonic setting of volcanic rocks from the Subpelagonian ophiolitic mélange in the Agoriani area (Othrys, Greece). Ofioliti, 28: 121-135.

Robertson A.H.F., 1994. Role of the tectonic facies concept in orogenic analysis and its application to Tethys in the Eastern Mediterranean region. Earth Sci. Review, 37: 139-213.

Robertson A.H.F., 2002. Overview of the genesis and emplacement of Mesozoic ophiolites in the Eastern Mediterranean Tethyan region. Lithos, 65: 1-67.

Robertson A.H.F. and Shallo M., 2000. Mesozoic-Tertiary tectonic evolution of Albania in its regional Eastern Mediterranean context. Tectonophysics, 316: 197-254.

Roelandts I. and Michel G., 1986. Sequential inductively coupled plasma determination of some rare earth elements in five French geostandards. Geostandards Newsletter, 10: 135-154.

Ross J.V. and Zimmerman J., 1996. Comparison of evolution and tectonic significance of the Pindos and Vourinos ophiolite suites, northern Greece. Tectonophysics, 256: 1-15.

Saccani E., Photiades A. and Padoa E., 2003. Geochemistry, petrogenesis and tectono-magmatic significance of volcanic and subvolcanic rocks from the Koziakas Mélange (Western Thessaly, Greece). Ofioliti, 28: 43-57.

Saccani E. and Photiades A., 2004. Mid-ocean ridge and suprasubduction affinities in the Pindos Massif ophiolites (Greece): implications for magma genesis in a proto-forearc setting. Lithos, 73: 229-253.

Saccani E., Padoa E. and Photiades A., 2004. Triassic mid-ocean ridge basalts from the Argolis Peninsula (Greece): new constraints for the early oceanization phases of the Neo-Tethyan Pindos basin. In: Dilek Y. and Robinson P.T. (Eds.) "Ophiolites in earth history", Geol. Soc. London Sp. Publ., 218: 109-127.

Shallo M., 1994. Outline of the Albanian Ophiolites: In: Beccaluva, L. (Ed.), Albanian ophiolites: State of the art and perspectives. Ofioliti, 19: 57-75.

Shervais J.W., 1982. Ti-V plots and the petrogenesis of modern ophiolitic lavas. Earth Planet. Sci. Letters, 59: 101-118.

Spray J.G. and Roddick J.C., 1980. Petrology and $^{40}Ar/^{39}Ar$ geochronology of some Hellenic sub-ophiolite metamorphic rocks. Contrib. Mineral. Petrol., 72: 43-55.

Spray J.G., Bébien J., Rex D.C. and Roddick J.C., 1984. Age constraints on the igneous and metamorphic evolution of the Hellenic-Dinaric ophiolites. In: J.E. Dixon and A.H.F. Robertson (Eds), The geological evolution of Eastern Mediterranean. Geol. Soc. London Sp. Publ., 17: 619-627.

Sun S.S. and McDonough W.F., 1989. Chemical and isotopic systematics of ocean basalts: Implications for mantle composition and processes. In: A.D. Saunders and M.J. Norry (Eds), Magmatism in the Ocean Basins. Geol. Soc. London Sp. Publ., 42: 313-346.

Taylor B. and Natland J., 1995. Active margin and marginal basin of the western Pacific. Am. Geophys. Union, Geophys. Monograph 88, Washington DC: 417 p.

Tatsumi Y. and Eggins S., 1995. Subduction zone magmatism. Blackwell Science, London, 211 pp.

Thuizat R., Whitechurch H., Montigny R. and Juteau T., 1981. K-Ar dating of some infra-ophiolitic metamorphic soles from the eastern Mediterranean: new evidence for oceanic thrusting before obduction. Earth and Planet. Sci. Letters, 52: 302-310.

Thy P. and Xenophontos C., 1991. Crystallization orders and phase chemistry of glassy lavas from the pillow sequences, Troodos Ophiolite, Cyprus. Jour. Petrol., 32: 403-428.

Uyeda S. and Kanamori H., 1979. Back-arc opening and the mode of subduction. J. Geophys. Res., 84: 1049-1061.

Walker D., Shibata T. and DeLong S.E., 1979. Abyssal Tholeiite from the Oceanographer Fracture Zone. II Phase equilibria and Mixing. Contrib. Mineral. Petrol., 70: 111-125.

Yumul G.P., 1996. Varying mantle source of supra-subduction zone ophiolites: REE evidence from the Zambales Ophiolite Complex, Luzon, Philippines. Tectonophysics, 262: 243-262.

Received, March 15, 2004
Accepted, May 15, 2004